induced CA release. These data suggest that AChE inhibitors extend the sites of action of endogenous ACh to the extra-synaptic regions of chromaffin cells.

In the exogenous ACh-induced CA release, AChE inhibitors enhanced the nicotinic receptor-mediated Epi and NE release and the muscarinic receptor-mediated Epi release, but did not affect the qualitative contribution of nicotinic or muscarinic receptors. On the other hand, in the endogenous ACh-induced CA release, AChE inhibitors not only enhanced the nicotinic receptor-mediated Epi and NE release, but also elicited the muscarinic receptor-mediated Epi release. These results indicate that AChE inhibitor not only elevates tissue ACh concentration by blocking decomposition of exogenous and endogenous ACh, but also extends the site of action of endogenous ACh to the extra-synaptic regions of chromaffin cells. This extension elicits the cholinergic transmission mediated through extra-synaptic muscarinic receptors of Epi-storing chromaffin cells.

5. CONCLUSION

Microdialysis technique with high-performance liquid chromatography makes it possible to continuously monitor Epi and NE release from *in vivo* rat adrenal medulla at 1min-intervals. In the rat adrenal gland, muscarinic receptors are present on the extra-synaptic region of the Epi-storing chromaffin cells, and AChE restricts this muscarinic receptor-mediated cholinergic transmission. Thus, a decrease in cholinesterase activity could not only enhance the nicotinic receptor-mediated Epi and NE release but also elicit the muscarinic receptor-mediated Epi release.

ACKNOWLEDGEMENT

This study was supported by grants in aid for scientific research from the Ministry of Education, Science, and Culture of Japan and by a grant from the Technology Agency, Encourage System of COE.

REFERENCES

1. T. Kimura, T. Shimamura, and S. Satoh, Effects of pirenzepine and hexamethonium on adrenal catecholamine release in responses to endogenous and exogenous acetylcholine in anesthetized dogs, *J. Cardiovasc. Pharmacol.* 20, 870-874 (1992).
2. A. R. Wakade, and T. D. Wakade, Contribution of nicotinic and muscarinic receptors in the secretion of catecholamines evoked by endogenous and exogenous acetylcholine, *Neuroscience* 10, 973-978 (1983).
3. T. Akiyama, and T. Yamazaki, Adrenergic inhibition of endogenous acetylcholine release on postganglionic cardiac vagal nerve terminals, *Cardiovasc. Res.* 46, 531-538 (2000).
4. T. Akiyama, and T. Yamazaki, Myocardial interstitial norepinephrine and dihydroxyphenylglycol levels during ischemia and reperfusion, *Cardiovasc. Res.* 49, 78-85 (2001).

THE JOURNAL OF BIOLOGICAL CHEMISTRY
Vol. 277, No. 26, Issue of June 28, pp. 23747–23754, 2002
Printed in U.S.A.

Sphingosine 1-Phosphate Induces Membrane Ruffling and Increases Motility of Human Umbilical Vein Endothelial Cells via Vascular Endothelial Growth Factor Receptor and CrkII*[S]

Received for publication, December 11, 2001, and in revised form, March 21, 2002
Published, JBC Papers in Press, April 15, 2002, DOI 10.1074/jbc.M111794200

Akira Endo‡, Ken-Ichiro Nagashima‡, Hitoshi Kurose§, Seibu Mochizuki¶, Michiyuki Matsuda‖, and Naoki Mochizuki‡**

From the ‡Department of Structural Analysis, National Cardiovascular Center Research Institute, Suita, Osaka 565-8565, the §Laboratory of Pharmacology and Toxicology, Graduate School of Pharmaceutical Science, University of Tokyo, Hongo, Bunkyo-ku, 113-0033, the ¶Division of Cardiology, Jikei University School of Medicine, Nishi-Shinbashi, Minato-ku, Tokyo 105-8461, and the ‖Department of Tumor Virology, Research Institute for Microbial Diseases, Osaka University, Osaka 565-0871, Japan

Sphingosine 1-phosphate (S1P), a ligand for endothelial differentiation gene family proteins, is one of the most potent signal mediators released from activated platelets. Here, we report that S1P induces membrane ruffling of human umbilical vein endothelial cells (HUVECs) via the vascular endothelial growth factor receptor (VEGFR), Src family tyrosine kinase(s), and the CrkII adaptor protein. S1P induced prominent phosphorylation of CrkII in HUVECs, indicating that CrkII was involved in the S1P-induced signaling pathway. S1P-induced CrkII phosphorylation was blocked by pertussis toxin and overexpression of the carboxyl terminus of β-adrenergic receptor kinase, indicating that the βγ subunit of G_i was required for the phosphorylation. Notably, the S1P-induced CrkII phosphorylation was also abolished by inhibitors of VEGFR or Src family tyrosine kinases. By using Picchu, a real time monitoring protein for CrkII phosphorylation, we found that S1P induced rapid CrkII phosphorylation at membrane ruffles. Finally, we observed that expression of a dominant negative mutant of CrkII inhibited the S1P-induced membrane ruffling and cell migration. These results delineated a novel S1P signaling pathway that involves sequential activation of G_i-coupled receptor(s), VEGFR, Src family tyrosine kinase(s), and the CrkII adaptor protein, and which is responsible for both the induction of membrane ruffling and the increase in cell motility.

Sphingosine 1-phosphate (S1P)[1] released from activated platelets (1) is a potent angiogenic factor of vascular endothelial cells. Angiogenesis requires endothelial cell proliferation and migration. S1P promotes proliferation and migration of endothelial cells through the endothelial differentiation gene (EDG) family of G protein-coupled receptors, EDG-1, -3, -5, -6, and -8 (2–6). S1P induces cytoskeletal reorganization that includes cortical actin rearrangement (7), focal adhesion assembly, and stress fiber formation (8, 9). In addition to these cytoskeletal changes, membrane ruffling is a renowned characteristic of migratory cells (10). Indeed, S1P reportedly promotes cell migration in endothelial cells expressing EDG-1 and -3 (11–13).

CrkII is an adaptor protein consisting of a Src homology 2 (SH2) domain and two SH3 domains (14). Alternative splicing of the human *crk* gene generates two Crk proteins, designated as CrkI and CrkII. CrkI lacks the carboxyl-terminal SH3 of CrkII. The SH2 domain of CrkII binds several phosphotyrosine-containing proteins, $p130^{Cas}$, paxillin, and Cbl, whereas the SH3 domain of CrkII binds to C3G, DOCK180, and Abl (15). Recently, CrkII associated with DOCK180 has received attention for its role in cell migration (16, 17).

The involvement of CrkII in cellular migration and the induction of membrane ruffling has been studied extensively both biochemically and genetically (15). The Crk-DOCK180-Rac pathway is conserved from nematode to man and plays a critical role in the regulation of membrane ruffling and cellular migration. We have shown that one of the two major Crk SH3-binding proteins, DOCK180, binds to and activates Rac1 and Rac2 to induce membrane ruffling (18, 19). A defect in *ced*-5, a homolog of *DOCK180*, inhibits migration of the distal tip cells and phagocytosis of apoptotic bodies (20, 21). It has been proven genetically that *ced*-5 is downstream from *ced*-2, a homolog of *crkII*, and upstream from *ced*-10, a homolog of *rac* (21). In *Drosophila melanogaster*, nonfunctional mutation in *myoblast city*, a homolog of DOCK180, results in the failure of dorsal closure (22), suggesting defective cell migration.

CrkII becomes phosphorylated on Tyr^{221} upon stimulation by the following growth factors: vascular endothelial growth factor (VEGF) (23), epidermal growth factor (EGF) (24), nerve growth factor (25), platelet-derived growth factor (PDGF) (26), and insulin-like growth factor I (27). Among these growth factors, VEGF induces the most prominent endothelial cell migration. Notably, CrkII is also phosphorylated upon S1P stimulation in NIH-3T3 cells (28), although the mechanisms by which CrkII is regulated downstream from the EDG receptor and how CrkII is

* This work was supported in part by grants from the Ministry of Health, Labor, and Welfare Foundation of Japan, from the Promotion of Fundamental Studies in Health Science of the Organization for Pharmaceutical Safety and Research of Japan, and from the Human Science Foundation of Japan. The costs of publication of this article were defrayed in part by the payment of page charges. This article must therefore be hereby marked "*advertisement*" in accordance with 18 U.S.C. Section 1734 solely to indicate this fact.

[S] The on-line version of this article (available at *http://www.jbc.org*) contains video files.

** To whom correspondence should be addressed: Dept. of Structural Analysis, National Cardiovascular Center Research Institute, 5-7-1 Fujishirodai, Suita, Osaka 565-8565, Japan. Tel.: 81-6-6833-5012 (ext. 2508); Fax: 81-6-6835-5461; E-mail: nmochizu@ri.ncvc.go.jp.

[1] The abbreviations used are: S1P, sphingosine 1-phosphate; BCECF-AM, 2′,7′-bis(2-carboxyethyl)-5-(6)-carboxyfluorescein acetoxymethyl ester; CSK, carboxyl-terminal Src kinase; EDG, endothelial differentiation gene; EGF, epidermal growth factor; EGFP, enhanced green fluorescent protein; EGFR, EGF receptor; ERK, extracellular signal-regulated kinase; $G_i\beta\gamma$, βγ subunits of G_i protein; HUVECs, human umbilical vein endothelial cells; IRES, internal ribosomal entry site; PDGF, platelet-derived growth factor; PDGFR, PDGF receptor; PTX, pertussis toxin; SH2 and SH3, Src homology 2 and 3, respectively; VEGF, vascular endothelial growth factor; VEGFR, VEGF receptor.

involved in cell migration have not yet been elucidated.

Among the many receptor tyrosine kinases, the VEGF receptor (VEGFR) is the one most highly expressed in vascular endothelial cells. VEGFR is required to develop a new vasculature by inducing endothelial cell migration and proliferation (29). The VEGFR family is composed of VEGFR-1 (Flt-1), VEGFR-2 (Flk-1 or KDR), and VEGFR-3 (Flt-4) (30).VEGFR-2 evokes a wide variety of biological responses, including endothelial cell proliferation and migration and increased cell permeability via SH2-containing signaling molecules, such as Src tyrosine kinase (31), phospholipase Cγ (32), and phosphatidylinositol 3-kinase (33). Recently, it has been reported that VEGFR-2 induces CrkII phosphorylation (23) and that VEGFR-1 provides a potential CrkII binding site on Tyr^{1333} (34).

This study investigates the molecular mechanism of S1P-induced endothelial cell migration. The results demonstrate that S1P induces CrkII phosphorylation by the βγ subunits of heterotrimeric G_i protein ($G_i\beta\gamma$)-mediated transactivation of VEGFR followed by the activation of Src family tyrosine kinase(s) and that CrkII is responsible for the membrane ruffling and cell motility induced by S1P in human umbilical vein endothelial cells (HUVECs).

EXPERIMENTAL PROCEDURES

Reagents and Antibodies—The following were purchased from Calbiochem (La Jolla, CA): AG1478, an inhibitor of EGF receptor (EGFR) kinase (35); AG1296, an inhibitor of PDGF receptor (PDGFR) kinase (36); AG1433 (37) and SU5614 (38), inhibitors of both PDGFR and VEGFR-2; VEGFR kinase inhibitor, an inhibitor of both VEGFR-1 and -2 kinases (39); PP2, an inhibitor of Src family tyrosine kinases (40); and pertussis toxin (PTX). Recombinant human $VEGF_{165}$ was purchased from R&D systems (Minneapolis), S1P from Biomol (Plymouth, PA), and basic fibroblast growth factor from Peprotech (London, UK). All other reagents were from Sigma. Anti-phospho-p44/42 mitogen-activated protein kinase (ERK) antibody and anti-EGFR antibody were from Cell Signaling Technology (Beverly, MA), anti-ERK antibody was from Upstate Technology (Lake Placid, NY), anti-phospho-VEGFR-2 was from Oncogene Research Products (Cambridge, MA), and anti-Crk antibody and anti-phosphotyrosine antibody (PY20) were from Transduction Laboratories (Lexington, KY).

Plasmids and Virus—cDNA coding CrkI replaced either at Arg^{38} by Val (hereafter, R38V) or at Trp^{169} by Leu (hereafter, W169L) was subcloned into the bicistronic promoter vector, pCXN2-FLAG-IRES-EGFP (41, 42). We produced a recombinant adenovirus for the *in vivo* CrkII phosphorylation-monitoring protein, Picchu (43), by means of an Adeno-X expression system (CLONTECH). Briefly, Picchu consists of a yellow emitting mutant of green fluorescent protein (YFP), CrkII, and a cyan emitting mutant of green fluorescent protein (CFP) from the amino terminus (43). Upon phosphorylation on Tyr in Picchu corresponding to Tyr^{221} of CrkII, SH2 binds to this phosphotyrosine, which causes intramolecular folding of Picchu and results in an increase in fluorescent resonance energy transfer from CFP to YFP. Adenovirus expressing both FLAG-tagged CrkI-W169L and EGFP was produced in a manner similar to that for adenovirus expressing Picchu. Recombinant adenovirus for the carboxyl terminus of β-adrenergic receptor kinase and for GFP was produced by the COS-TPC method as described previously (44). Adenovirus for carboxyl-terminal Src kinase (CSK) was obtained from S. Tanaka (University of Tokyo, Japan) (45).

Cells—HUVECs and COS-1 cells were purchased from American Type Culture Collection (Rockville, MD). HUVECs were cultured with Dulbecco's modified Eagle's medium supplemented with 10% fetal bovine serum, 2 mM L-glutamine, 0.1 mg/ml heparin, and 0.03 mg/ml endothelial cell growth supplement from Sigma, and used for experiments before passage 5. COS-1 cells were cultured in Dulbecco's modified Eagle's medium supplemented with 10% fetal bovine serum. HUVECs cultured on a collagen-coated 35-mm diameter glass base dish (Asahi Techono Glass Co., Tokyo) were transfected with 3 μg of plasmid DNA using LipofectAMINE PLUS Reagent (Invitrogen Corp.) or infected with adenovirus at the appropriate multiplicity of infection for more than 24 h before the stimulation with reagents for imaging.

Immunoprecipitation and Immunoblotting—HUVECs in 10-cm plates or COS-1 cells in six-well dishes were starved for 8 h and stimulated with reagents with or without pretreatment as indicated in the figure legends. Cells were exposed to the reagents at 37 °C for the time indicated in the figures, washed with buffered saline containing 10 mM Tris-HCl (pH 7.5) and 1 mM Na_3VO_4, and lysed in a lysis buffer (10 mM Tris-HCl (pH 7.5), 50 mM NaCl, 50 mM NaF, 1% Triton X-100, 5 mM EDTA, 2 mM Na_3VO_4, 0.1% bovine serum albumin, 20 μg/ml aprotinin, 1 mM phenylmethlysulfonyl fluoride), and cleared by centrifugation at 15,000 × *g* for 15 min. Aliquots of total cell lysate were subjected to immunoblotting with antibodies as indicated in the figures. The remaining lysate was subjected to immunoprecipitation using antibodies as indicated in the figures and protein A and G-Sepharose (Calbiochem), followed by SDS-PAGE and immunoblotting. Proteins reacting with primary antibodies were visualized by the ECL system (Amersham Biosciences, Buckinghamshire, UK) detecting peroxidase-conjugated secondary antibodies and analyzed with the LAS-1000 system (Fuji Film, Tokyo).

Quantitation of CrkII Phosphorylation—The intensities of the phosphorylated slower migrating form and nonphosphorylated faster migrating form of CrkII (24) were measured with an LAS-1000 image analyzer. Then, the percentage of the phosphorylated form was calculated for each sample. The ligand-induced increase in the phosphorylated CrkII was determined as the ratio to the control (prestimulation). Data from at least three independent experiments were averaged, and statistical significance was evaluated by Student's *t* test.

Fluorescent Resonance Energy Transfer Imaging—HUVECs infected with adenovirus for Picchu on a collagen-coated 35-mm diameter glass base dish were starved for 8 h and stimulated with 100 nM S1P. Cells were imaged on an Olympus IX-70 inverted microscope with a 75-W xenon arc lamp equipped with a MultiSpec Micro-Imager (Optical Insights, Santa Fe, NM) and a cooled CCD camera, CoolSNAP-HQ, controlled by MetaFluor (Roper Scientific, Trenton, NJ). CFP and YFP images were obtained simultaneously by a filter set consisting of an XF1071 excitation filter and an XF2034 dichroic mirror (Omega Optical, Inc., Brattleboro, VT). The emission ratio of YFP to CFP and the intensity of CFP were used for imaging of the phosphorylation of Picchu in the intensity modulated display mode controlled by MetaFluor.

Time-lapse Imaging, Quantitative Analysis of Membrane Ruffling, and Cell Motility Analysis—HUVECs transfected with either pCXN2-FLAG-CrkI-W169L-IRES-EGFP or pCXN2-FLAG-CrkI-R38V-IRES-EGFP were starved for 8 h and stimulated with S1P. A phase contrast image and a fluorescence image were recorded first, and then a sequential phase-contrast image was obtained every 30 s. A series of time-lapse images was converted to a video using MetaMorph 4.6 software (Roper Scientific). S1P-induced membrane extension reflecting the membrane ruffling was quantitated by measuring the cell size before and after S1P stimulation. The cell size was analyzed by a region measurement tool included in the MetaMorph 4.6 software. Cell motility was analyzed as described previously (46). Briefly, HUVECs labeled with BCECF-AM (Molecular Probes, Eugene, OR) were spread on a collagen-coated glass-base dish and cultured in Dulbecco's modified Eagle's medium supplemented with 1% fetal bovine serum for 2 h before exposure to S1P in the presence or absence of AG1433. HUVECs infected with either adenovirus expressing GFP or adenovirus expressing both CrkI-W169L and EGFP were spread and stimulated with S1P. Cells labeled with BCECF-AM or expressing EGFP were tracked by a series of time-lapse images using fluorescent microscopy. The distance between the point at which the cell attached and the end point to which the cell moved was measured by tracing cells. The velocity was obtained as the distance divided by the period during tracing of cells and was analyzed by a cell tracking system included in the MetaMorph 4.6 software.

RESULTS

CrkII Is Phosphorylated upon S1P and VEGF Stimulation in HUVECs—To explore the involvement of CrkII in S1P-induced migration of HUVECs, we examined whether CrkII became phosphorylated when HUVECs were stimulated with S1P. We have shown previously that the phosphorylated form of CrkII migrates more slowly than the wild-type CrkII on SDS-polyacrylamide gel (24). In the present study, we used this observation to detect the percentage of phospho-CrkII by SDS-PAGE, immunoblotting, and densitometry. In parallel, as a second measure of S1P stimulation, we also examined the S1P-induced activation of ERK by anti-phospho-ERK antibody. 100 nM S1P induced a statistically significant increase in level of phosphorylation of CrkII ($p < 0.01$) (Fig. 1*A*), and this con-

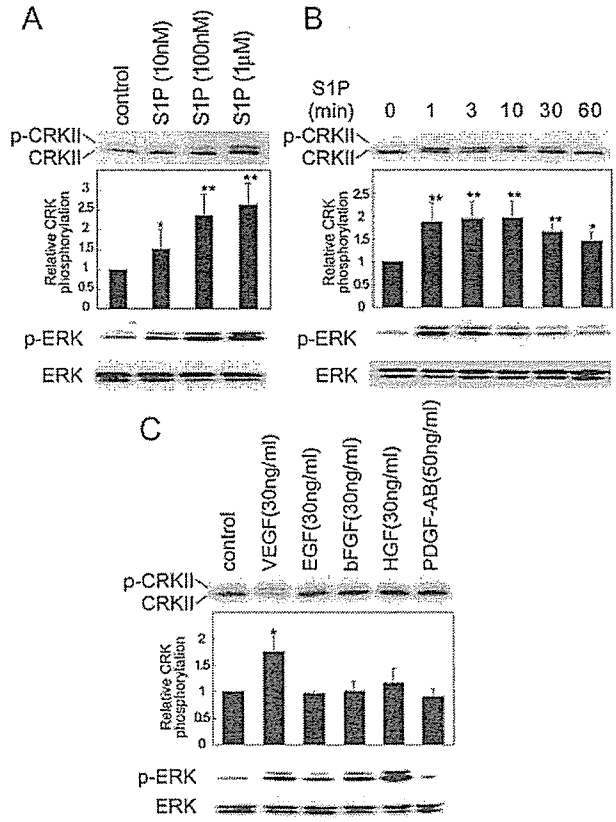

FIG. 1. **CrkII and ERK phosphorylation by S1P and VEGF in HUVECs.** *A*, HUVECs were stimulated at the concentration indicated at the *top* of the figure. Equal amounts of cell lysate were subjected to SDS-PAGE and immunoblotted with antibodies as indicated on the *left*. Phosphorylated CrkII (*p-CRKII*) and nonphosphorylated CrkII (*CRKII*) were detected as slower and faster migrating forms of CrkII on the membrane probed with anti-Crk antibody. *Relative CRK phosphorylation* indicates the ratio of the poststimulation p-CrkII fraction of total Crk (Crk + p-CrkII) to the prestimulation (control) p-CrkII fraction. The mean relative Crk phosphorylation is shown ± the S.D. Each immunoblot result is a representative of at least three independent experiments. A significant difference from the control by *t* test is indicated as an *asterisk* ($p < 0.05$) or *double asterisk* ($p < 0.01$). *B*, cells were exposed to 100 nM S1P for the duration indicated at the *top* of the figure and analyzed as in *A*. *C*, HUVECs were exposed to a series of growth factors as indicated at *top* for 5 min and analyzed by immunoblotting as in *A*. *p-Erk*, phospho-ERK; *bFGF*, basic fibroblast growth factor; *HGF*, hepatocyte growth factor; *PDGF-AB*, platelet-derived growth factor A-chain/B-chain heterodimer.

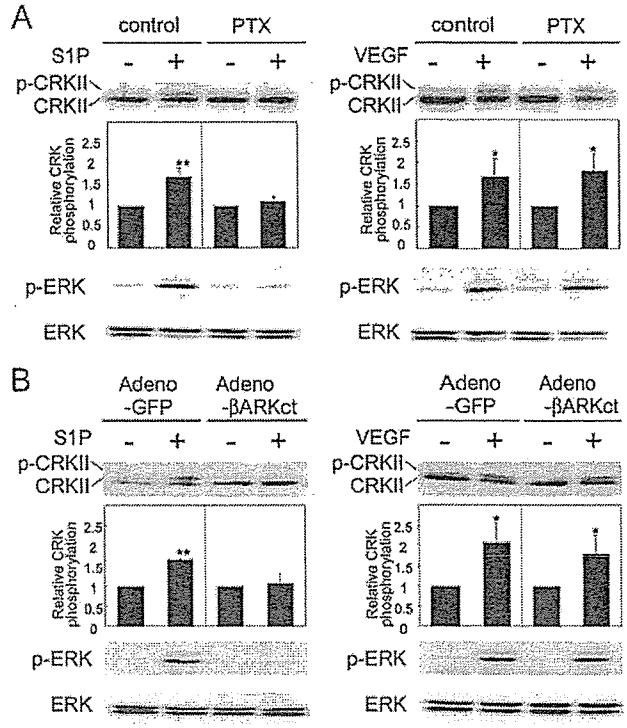

FIG. 2. **CrkII and ERK are phosphorylated in a $G_i\beta\gamma$-dependent manner upon S1P stimulation in HUVECs.** *A*, HUVECs pretreated with 50 ng/ml PTX for 8 h then starved for 8 h were stimulated with 100 nM S1P (*left panel*) or 30 ng/ml VEGF (*right panel*). Cell lysates were analyzed by immunoblotting, as described in the legend of Fig. 1. *B*, HUVECs infected with adenovirus expressing GFP (*Adeno-GFP*) or the carboxyl terminus of β-adrenergic receptor kinase (*Adeno-βARKct*) for 24 h were stimulated with S1P (*left panel*) or VEGF (*right panel*). Relative Crk phosphorylation was analyzed as described in the legend of Fig. 1.

centration was used in subsequent experiments. Upon S1P stimulation, phosphorylation of CrkII and ERK reached a plateau within 1 min and returned slowly to the basal level in 1 h (Fig. 1*B*). Both CrkII and ERK were phosphorylated in a dose- and time-dependent manner upon S1P stimulation in HUVECs. Because G protein-coupled receptors often transactivate receptor-type tyrosine kinases, we searched for growth factors that could induce CrkII phosphorylation in HUVECs. Among VEGF, EGF, basic fibroblast growth factor, hepatocyte growth factor, and PDGF, only VEGF induced significant CrkII phosphorylation (Fig. 1*C*). All growth factors except PDGF induced ERK phosphorylation, suggesting that VEGFR might be the tyrosine kinase receptor responsible for S1P-induced CrkII phosphorylation in HUVECs.

CrkII Phosphorylation Is G_i-dependent in HUVECs—To test which heterotrimeric G protein was involved in S1P-induced CrkII phosphorylation in HUVECs, we treated HUVECs with PTX before stimulation. Both CrkII and ERK phosphorylation by S1P were abolished by PTX pretreatment (Fig. 2*A*, *left panel*), indicating that S1P induced phosphorylation of CrkII and ERK via G_i. As expected, VEGF-dependent phosphorylation of CrkII and ERK was not affected by PTX (Fig. 2*A*, *right panel*). In addition, adenoviral-mediated overexpression of the carboxyl terminus of β-adrenergic receptor kinase, which sequesters βγ subunits (47), inhibited S1P-induced phosphorylation of CrkII and ERK. Adenoviral GFP, as a negative control, did not inhibit S1P-induced CrkII and ERK phosphorylation (Fig. 2*B*, *left panel*). Neither GFP nor the carboxyl terminus of β-adrenergic receptor kinase affected VEGF-induced phosphorylation of CrkII and ERK (Fig. 2*B*, *right panel*). These data indicated that both CrkII and ERK were phosphorylated downstream from $G_i\beta\gamma$ in HUVECs.

Src Family Tyrosine Kinases Are Involved in S1P-induced CrkII Phosphorylation in HUVECs—It has been shown that Src family tyrosine kinase(s) is required to transactivate EGFR in COS cells (48). Therefore, we examined the involvement of Src family tyrosine kinase(s) in S1P-induced CrkII phosphorylation in HUVECs by using a Src family tyrosine kinase inhibitor, PP2, and CSK, a tyrosine kinase that down-regulates Src activity. Pretreatment of HUVECs with PP2 blocked S1P-induced CrkII phosphorylation but not ERK phosphorylation (Fig. 3*A*, *left panel*). That Src family tyrosine kinase(s) was required for S1P-induced CrkII phosphorylation was confirmed by the expression of CSK (Fig. 3*B*, *left panel*). Surprisingly, VEGF-induced CrkII phosphorylation was also inhibited by PP2 and CSK (Fig. 3, *A*, *right panel* and *B*, *right panel*). Thus, Src family tyrosine kinase(s) appeared to function downstream

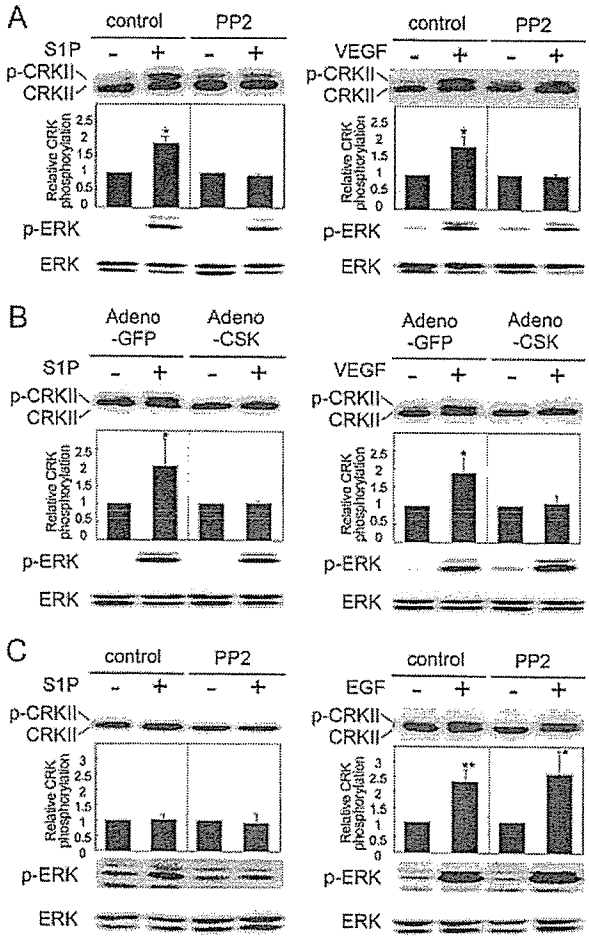

FIG. 3. **Src family tyrosine kinases are involved in phosphorylation of CrkII but not in ERK activation upon S1P stimulation in HUVECs.** *A*, HUVECs were pretreated with 20 nM PP2 for 20 min prior to stimulation with S1P (*left panel*) or VEGF (*right panel*) and analyzed for CrkII and ERK phosphorylation, as described in the legend of Fig. 1. *B*, HUVECs infected with adenovirus expressing GFP (*Adeno-GFP*) or adenovirus expressing CSK (Adeno-CSK) for 24 h were starved for 8 h and exposed to S1P (*left panel*) or VEGF (*right panel*). *C*, COS-1 cells pretreated with PP2 were exposed to S1P (*left panel*) or EGF (*right panel*) and analyzed for CrkII and ERK phosphorylation. Relative Crk phosphorylation was analyzed as described in the legend of Fig. 1.

from VEGFR in S1P-induced CrkII phosphorylation in HUVECs. In contrast to HUVECs, S1P did not induce CrkII phosphorylation (Fig. 3*C*, *left panel*), and Src family tyrosine kinases were not involved in EGF-induced CrkII phosphorylation (Fig. 3*C*, *right panel*) in COS-1 cells, although Src family tyrosine kinases were required for S1P-induced ERK phosphorylation (Fig. 3*C*, *left panel*).

EGFR Is Not Required for S1P-induced CrkII Phosphorylation in HUVECs—To exclude the involvement of EGFR in S1P-induced CrkII phosphorylation in HUVECs, HUVECs were pretreated with AG1478, an EGFR kinase inhibitor, before S1P stimulation. As expected, in the presence of AG1478 neither CrkII nor ERK phosphorylation was inhibited upon S1P stimulation in HUVECs (Fig. 4*A*, *left panel*). The inhibition of EGFR by AG1478 in HUVECs was confirmed by examining the EGF-induced ERK phosphorylation (Fig. 4*A*, *right panel*). In COS-1 cells, S1P-dependent (Fig. 4*B*, *left panel*) and EGF-dependent (Fig. 4*B*, *right panel*) phosphorylation of ERK were abrogated by pretreatment with AG1478, consistent with previous reports that EGFR is transactivated by G_i to activate

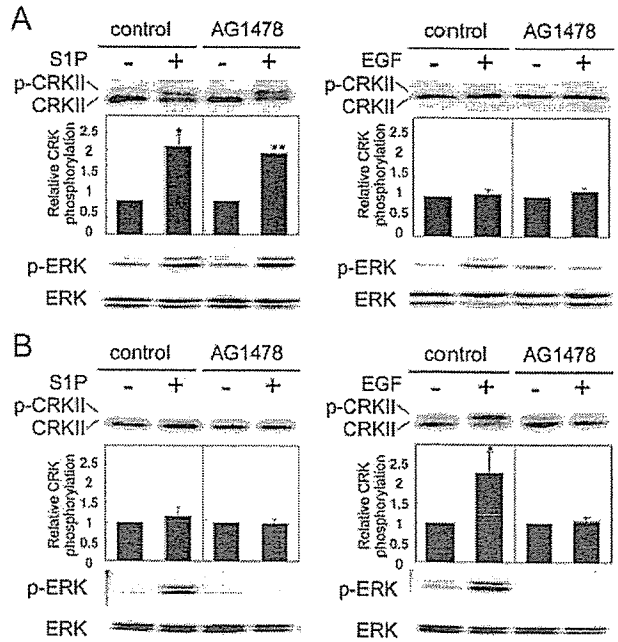

FIG. 4. **EGFR-independent CrkII and ERK phosphorylation by S1P in HUVECs.** *A*, HUVECs were pretreated with 10 nM AG1478 for 20 min prior to S1P (*left panel*) or EGF (*right panel*) stimulation. CrkII and ERK phosphorylation were analyzed as described in the legend of Fig. 1. *B*, COS-1 cells were analyzed as in *A*.

ERK (48, 49).

VEGFR but Not EGFR Is Transactivated in S1P-stimulated HUVECs—We examined whether the EGFR and the VEGFR were phosphorylated upon S1P stimulation in HUVECs. Only VEGFR-2 was phosphorylated upon S1P stimulation in HUVECs (Fig. 5, *top* and *middle panel*). Although VEGFR-1 and -2 are expressed in HUVECs (29), we could not test whether VEGFR-1 was phosphorylated because there was no specific and sensitive antibody to VEGFR-1 available for this analysis. In contrast to VEGFR-2, EGFR was phosphorylated in S1P-stimulated COS-1 cells (Fig. 5, *bottom panel*) but not in S1P-stimulated HUVECs (Fig. 5, *top panel*), suggesting that the S1P-induced EGFR activation was cell type-specific.

VEGFR Is Required for S1P-induced CrkII Phosphorylation—We further confirmed that VEGFR was responsible for the S1P-induced CrkII phosphorylation by the use of three VEGFR inhibitors. AG1433 and SU5614 inhibit the tyrosine kinase activity of VEGFR-2 and PDGFR, whereas VEGF-tyrosine kinase inhibitor is a specific inhibitor for VEGFR-1 and -2. As expected, all of these inhibitors blocked S1P-induced phosphorylation of CrkII but not that of ERK (Fig. 6*A*, *upper panel*). VEGF-induced ERK phosphorylation in HUVECs was completely inhibited by the VEGFR inhibitors (Fig. 6*A*, *lower panel*), demonstrating the effectiveness of these compounds. As an additional control, we also tested AG1296, an inhibitor specific for PDGFR, which would not be expected to inhibit S1P signaling to ERK and CrkII (Fig. 1*C*). As expected, AG1296 did not abrogate phosphorylation of either ERK or CrkII upon S1P stimulation (Fig. 6*B*, *left panel*). The inability of AG1296 to inhibit VEGFR signaling was also confirmed (Fig. 6*B*, *right panel*). Therefore, although we cannot exclude the involvement of VEGFR-1 without a VEGFR-1-specific inhibitor, S1P-induced CrkII phosphorylation required VEGFR-2. In contrast to CrkII phosphorylation, S1P-induced ERK phosphorylation was mediated mostly by VEGFR-independent pathway(s).

CrkII Phosphorylation at the Membrane Ruffling—To examine where and when CrkII was involved in S1P-induced mem-

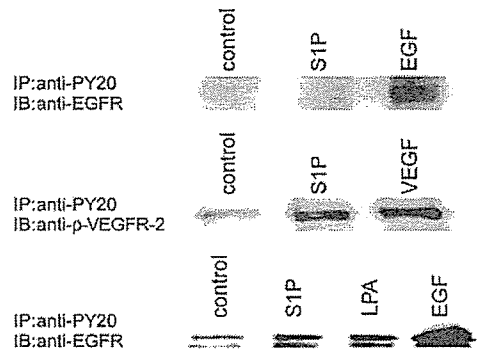

FIG. 5. **Transactivation of VEGFR by S1P but not EGFR in HUVECs.** HUVECs (*top* and *middle panels*) and COS-1 cells (*bottom panel*) stimulated as indicated at the *top* of the figure were immunoprecipitated (*IP*) with PY20 followed by immunoblotting (*IB*) with anti-EGFR antibody (*top panel*), anti-phospho-VEGFR-2 antibody (*middle panel*), and anti-EGFR antibody (*bottom panel*), respectively. Immunoblots are representative of at least three independent experiments. *LPA*, lysophosphatidic acid.

brane ruffling, we used the phosphorylation indicator of the Crk chimeric unit, Picchu, for monitoring CrkII phosphorylation on Tyr^{221} in living HUVECs. Phosphorylation of CrkII, shown by *red* hues, was most prominent at membrane ruffles in HUVECs after S1P stimulation (Fig. 7*A* and supplemental material). Similar phosphorylation of CrkII at membrane ruffles was also observed in VEGF-stimulated HUVECs (Fig. 7*B* and supplemental material). The intensity of Picchu, which reflects the concentration of CrkII, was increased at membrane ruffles. These observations indicated that CrkII was recruited to and phosphorylated at membrane ruffles upon S1P stimulation.

VEGFR Is Required for S1P-induced Membrane Ruffling and Cell Motility—To examine the requirement of VEGFR, we tested the effect of AG1433, an inhibitor for VEGFR kinase, on membrane ruffling and cell motility upon S1P stimulation (Fig. 8). HUVECs responded to S1P and showed prominent membrane ruffling (Fig. 8*A*, *upper panel*, and supplemental material), whereas HUVECs pretreated with AG1433 showed less membrane ruffling upon S1P stimulation (Fig. 8*A*, *lower panel*, and supplemental material). Because S1P-induced membrane ruffling was accompanied by spreading of the peripheral plasma membrane, we quantitated the effect of AG1433 by measuring the area of cells. S1P increased cell size by about 30%. This S1P-induced increase in cell size was completely inhibited by AG1433 (Fig. 8*A*, *right panel*). Furthermore, we examined the effect of AG1433 on S1P-induced cell motility of HUVECs stimulated with S1P (Fig. 8*B*). S1P accelerated the migratory velocity of HUVECs (Fig. 8*B*, *left* and *center panel*); however, this acceleration was inhibited by pretreatment with AG1433 (Fig. 8*B*, *right* and *center panel*). These results suggested that VEGFR was required for S1P-induced membrane ruffling and cell motility.

CrkII Is Required for S1P-induced Membrane Ruffling and Cell Motility—To examine whether CrkII was required for S1P-induced membrane ruffling and cell motility, we used dominant negative mutants of CrkI, CrkI-W169L and CrkI-R38V. CrkI is a splicing variant of CrkII and lacks the carboxyl-terminal SH3 domain. CrkI-W169L consists of an intact SH2 and a nonfunctioning SH3 domain. CrkI-R38V consists of a nonfunctioning SH2 and an intact SH3 domain. We have shown previously that CrkI-W169L and CrkI-R38V work as dominant negative mutants for CrkI/II (42, 50). Phosphorylation of CrkII upon S1P stimulation was abolished by adenovirus-mediated overexpression of CrkI-W169L (Fig. 9*A*, *left panel*). In addition, VEGF-induced CrkII phosphorylation was completely inhibited by overexpression of CrkI-W169L (Fig. 9*A*, *right panel*), suggesting that Crk functioned downstream from VEGFR. Furthermore, HUVECs transfected with CrkI-W169L did not show any membrane ruffling after S1P stimulation (Fig. 9*B* and supplemental material). Overexpression of CrkI-R38V also inhibited S1P-induced membrane ruffling (data not shown). Finally, we examined the effect of overexpression of CrkI-W169L on cell motility of HUVECs. S1P accelerated the migratory velocity of HUVECs infected with the control adenovirus, Adeno-GFP (Fig. 9*C*, *left* and *center panel*); however, the S1P-induced acceleration of migration was completely abolished by the adenovirus carrying the dominant negative CrkI-W169L gene (Fig. 9*C*, *center* and *right panel*). These observations indicated that CrkII was required for S1P-induced membrane ruffling and cell migration.

DISCUSSION

Angiogenesis, which is observed in wound repair, tumorigenesis, and tissue ischemia, is an integral feature of vascular sprouting, branching, and remodeling and is coordinated by endothelial cells, vascular smooth muscle cells, and mesenchymal cells (51). VEGF, angiopoietin, and ephrin have been shown to be key molecules in the promotion of angiogenesis via activation of the VEGFR, Tie, and Eph expressed on vascular endothelial cells, respectively (51). Recently, S1P has been identified as another potent angiogenic factor because it promotes prominent endothelial cell migration (11, 52, 53). However, despite these extensive studies, the molecular mechanism of S1P-induced endothelial cell migration is not yet clearly understood. In this study, we delineate a novel signaling pathway required for S1P-triggered cell migration via sequential activation of $G_i\beta\gamma$, VEGFR, Src family tyrosine kinase(s), and CrkII.

Our data support the idea that CrkII is involved in the S1P-stimulated signaling pathway in HUVECs. CrkII was phosphorylated upon S1P stimulation in HUVECs, indicating that CrkII functions downstream from the EDG receptor in HUVECs, just as it functions downstream from nerve growth factor receptors in PC12 cells and EGFR in NRK cells in response to nerve growth factor and EGF, respectively (24, 25). To explore where and how CrkII functions, we monitored CrkII phosphorylation in S1P-stimulated HUVECs by Picchu, which reflects CrkII phosphorylation on Tyr^{221}. Our data showed that CrkII was phosphorylated at the site of membrane ruffling. CrkII was also localized in newly assembling focal complexes at the leading edge, where CrkII was likely to bind to $p130^{Cas}$ upon S1P stimulation.[2] In addition, it has been reported that $p130^{Cas}$ and CrkII are colocalized at membrane ruffles upon S1P stimulation (9) and that the CrkII and $p130^{Cas}$ complex functions as a critical molecular switch in directing the membrane ruffling and cell migration (16). Our results together with these reports suggest that CrkII is involved in S1P-induced membrane ruffling in HUVECs. Furthermore, the inhibition of S1P-induced membrane ruffling and cell motility by the dominant negative mutant of CrkII supports our proposal. Because Rac activation via the CrkII·DOCK180 complex has already been demonstrated both biochemically and genetically (18, 20, 21), our finding connects the S1P signal transduction cascade to the actin reorganization machinery via Rac.

The present study is the first to demonstrate transactivation of VEGFR and thereby to link G_i-coupled EDG receptors to CrkII phosphorylation. S1P-induced CrkII phosphorylation is dependent upon PTX and $\beta\gamma$ subunits. This observation suggests that among the eight EDG family proteins, those coupled

[2] A. Endo and N. Mochizuki, unpublished results.

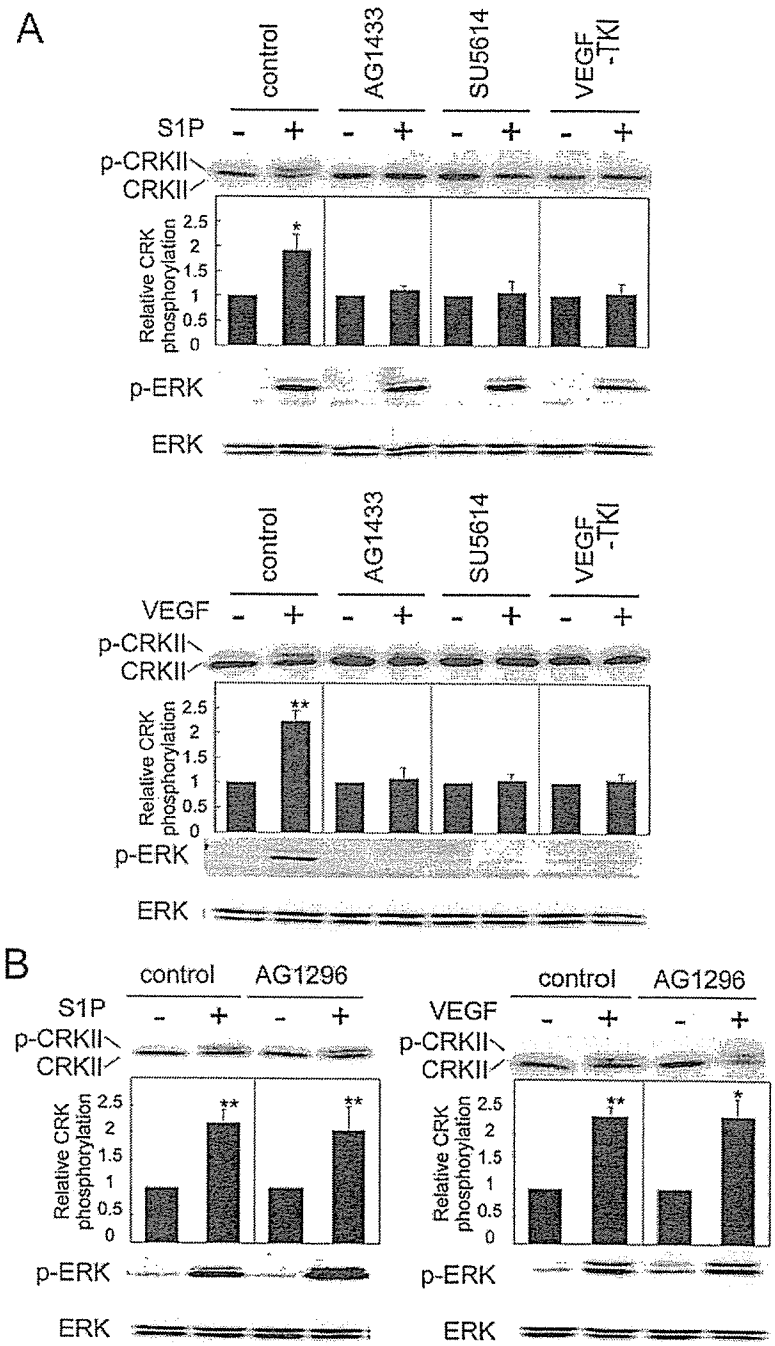

FIG. 6. **VEGFR-mediated CrkII phosphorylation upon S1P stimulation in HUVECs.** *A*, HUVECs pretreated with a tyrosine kinase inhibitor, 20 μM AG1433, 10 μM SU5614, or 5 μM VEGF-TKI, were exposed to S1P (*upper panel*) or VEGF (*lower panel*) and analyzed as described in the legend of Fig. 1. VEGF-TKI is an inhibitor of both VEGFR-1 and -2. *B*, HUVECs pretreated with 10 μM AG1296, a PDGF-specific inhibitor, were exposed to S1P (*left panel*) or VEGF (*right panel*) and analyzed as in *A*.

with G_i are responsible for the CrkII phosphorylation in HUVECs. Such candidates in HUVECs are EDG-1 and -3 (11, 54). Many G_i-coupled receptors are known to transactivate EGFR and PDGFR in various cell types and in response to a wide variety of ligands (49, 55). These two tyrosine kinase receptors are, to the best of our knowledge, the only two receptors identified in G_i-mediated transactivation. The transactivation of EGFR was first reported in Rat-1 fibroblasts stimulated with endothelin-1, lysophosphatidic acid, or thrombin (56). PDGFR is also transactivated by angiotensin II in vascular smooth muscle cells (57) and by dopamine in CHO-K1 cells (58).

In contrast to other cell types, there was no evidence that the EGFR and the PDGFR are involved in S1P signaling in HUVECs. EGFR was not tyrosine-phosphorylated upon S1P stimulation. The EGFR inhibitor AG1478 did not abrogate either CrkII phosphorylation or ERK activation upon S1P stimulation. In addition, PDGFR may not be expressed in HUVECs, as suggested by the findings that ERK was not activated by PDGF stimulation and that S1P-stimulated CrkII phosphorylation was not abrogated by a PDGFR inhibitor. Recently, heparin-binding EGF, a membrane-bound EGF-like ligand, has been shown to transactivate EGFR in COS cells stimulated with lysophosphatidic acid (55) and in vascular smooth muscle cells stimulated with angiotensin II (59). If this is a general mechanism for the transactivation of receptor tyrosine kinases, VEGF, which is the only inducer for CrkII phosphorylation tested in this study, may be released from the cell membrane of S1P-stimulated HUVECs.

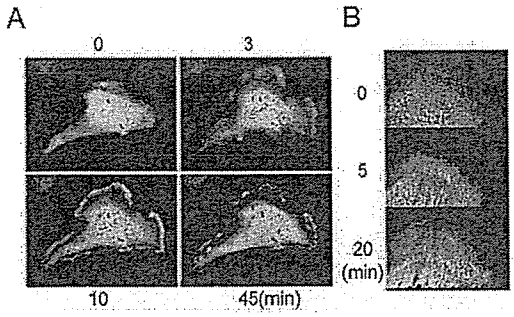

FIG. 7. **Spatio-temporal imaging of phosphorylation of CrkII upon S1P stimulation in HUVECs.** *A*, HUVECs infected with adenovirus expressing Picchu were stimulated with 100 nM S1P. The emission ratio of YFP to CFP and the intensity of CFP were used for imaging of phosphorylation of Picchu in the intensity modulated display mode. *Red* and *blue* hues indicate high and low emission ratio, respectively. The intensity of each hue reflects the intensity of the fluorescence from CFP of Picchu. *B*, HUVECs expressing Picchu were stimulated with VEGF, and the membrane ruffles were magnified. Representative intensity modulated display images are shown.

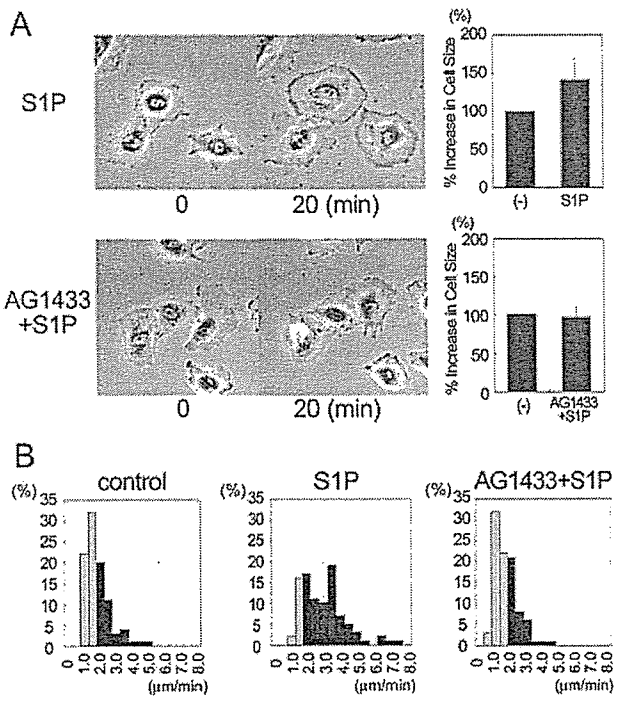

FIG. 8. **VEGFR is required for S1P-promoted membrane ruffling and cell motility.** *A*, HUVECs were stimulated with 100 nM S1P for 20 min in the absence or presence of 20 μM AG1433, an inhibitor for VEGFR kinase. Cells were imaged before and after S1P stimulation (*left panels*). The percent increase in cell size was analyzed by measuring the cell area before and after S1P stimulation in the absence or presence of AG1433 using a measurement tool included in the MetaMorph 4.6 software (*right bar graph*). *B*, HUVECs labeled with fluorescein were unstimulated (*left panel*), stimulated with S1P (*center panel*), or stimulated with S1P in the presence of AG1433 (*right panel*). 100 cells were monitored for 6 h after stimulation, and their velocities were calculated using a cell tracking program. Cells moving faster than 1.5 μm/min are shown in the *black* column. Cell labeling and velocity calculation were performed as described under "Experimental Procedures."

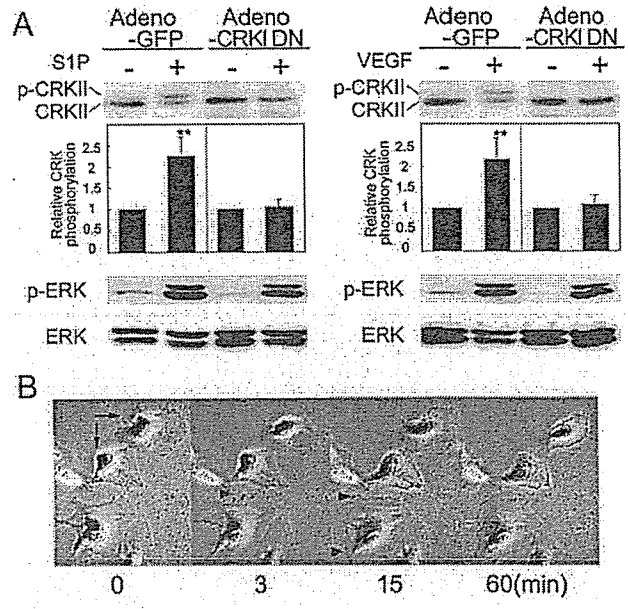

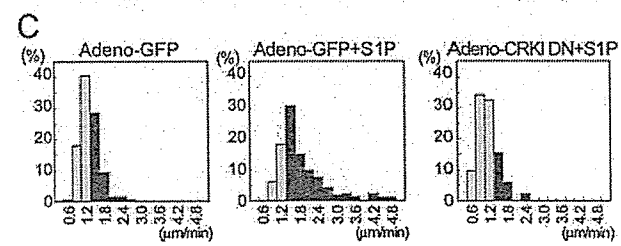

FIG. 9. **Crk is required for S1P-promoted membrane ruffling and cell motility of HUVECs.** *A*, HUVECs infected with either adenovirus expressing GFP (*Adeno-GFP*) or both CrkI-W169L and EGFP (*Adeno-CRKI DN*) were stimulated with 100 nM S1P (*left panel*) or 30 ng/ml VEGF (*right panel*) and analyzed as described in the legend of Fig. 1. *B*, HUVECs transfected with pCXN2-FLAG-CrkI-W169L-IRES-EGFP (indicated by the *arrows*) and untransfected HUVEC were stimulated with 100 nM S1P. The phase contrast image and epifluorescent image for EGFP are shown overlaid at time 0 (min). Cells were exposed to S1P for the period indicated at the *bottom* of the figure. A representative overlaid image before SIP stimulation and phase contrast images after S1P stimulation are shown. *Arrowheads* indicate the membrane ruffling. *C*, HUVECs infected with adenovirus expressing GFP were unstimulated (*left panel*) or stimulated with S1P (*center panel*). Those infected with adenovirus expressing both CrkI-W169L and EGFP were stimulated with S1P (*right panel*). 150 cells were monitored for 6 h after stimulation, and their velocities were calculated using a cell tracking program included in the MetaMorph 4.6 software. Cells moving faster than 1.5 μm/min are shown in the *black* column.

We have shown that activation of VEGFR and subsequent activation of Src family tyrosine kinase(s) are required for S1P-induced CrkII phosphorylation in HUVECs. We have not identified which of the VEGFR family proteins plays the principal role in the CrkII phosphorylation because antibodies highly specific to each of the VEGFR family proteins are not yet available. VEGFR-2 was phosphorylated by S1P, and CrkII phosphorylation was abolished by VEGFR-2 inhibitors. In addition, CrkII phosphorylation upon either VEGF or S1P stimulation was inhibited by CSK and PP2, indicating that VEGFR indirectly induces CrkII phosphorylation. Furthermore, S1P-promoted membrane ruffling and cell motility were diminished by an inhibitor for VEGFR-2. This is consistent with the previous finding that VEGFR-2 is responsible for migration of HUVECs (60). Thus, among VEGFR family proteins, VEGFR-2 appears to be a candidate for S1P-induced CrkII phosphorylation and increase in motility of HUVECs.

In conclusion, we have delineated a novel S1P signaling pathway involving a sequential activation of G_i-coupled receptor(s), VEGFR, Src family tyrosine kinase(s), and the CrkII adaptor protein. Furthermore, we have demonstrated that this novel signaling pathway is responsible for the membrane ruffling and for the increase in cell motility.

Acknowledgments—We thank S. Tanaka for the adenovirus for CSK, Howard K. Surks for helpful input, and M. Sone and H. Shimamoto for technical assistance.

REFERENCES

1. Yatomi, Y., Yamamura, S., Ruan, F., and Igarashi, Y. (1997) *J. Biol. Chem.* **272,** 5291–5297
2. Lee, M. J., Van Brocklyn, J. R., Thangada, S., Liu, C. H., Hand, A. R., Menzeleev, R., Spiegel, S., and Hla, T. (1998) *Science* **279,** 1552–1555
3. Van Brocklyn, J. R., Tu, Z., Edsall, L. C., Schmidt, R. R., and Spiegel, S. (1999) *J. Biol. Chem.* **274,** 4626–4632
4. Yamazaki, Y., Kon, J., Sato, K., Tomura, H., Sato, M., Yoneya, T., Okazaki, H., Okajima, F., and Ohta, H. (2000) *Biochem. Biophys. Res. Commun.* **268,** 583–589
5. Yamaguchi, F., Tokuda, M., Hatase, O., and Brenner, S. (1996) *Biochem. Biophys. Res. Commun.* **227,** 608–614
6. Im, D. S., Heise, C. E., Ancellin, N., O'Dowd, B. F., Shei, G. J., Heavens, R. P., Rigby, M. R., Hla, T., Mandala, S., McAllister, G., George, S. R., and Lynch, K. R. (2000) *J. Biol. Chem.* **275,** 14281–14286
7. Garcia, J. G., Liu, F., Verin, A. D., Birukova, A., Dechert, M. A., Gerthoffer, W. T., Bamberg, J. R., and English, D. (2001) *J. Clin. Invest.* **108,** 689–701
8. Wang, F., Nobes, C. D., Hall, A., and Spiegel, S. (1997) *Biochem. J.* **324,** 481–488
9. Ohmori, T., Yatomi, Y., Okamoto, H., Miura, Y., Rile, G., Satoh, K., and Ozaki, Y. (2001) *J. Biol. Chem.* **276,** 5274–5280
10. Lauffenburger, D. A., and Horwitz, A. F. (1996) *Cell* **84,** 359–369
11. Wang, F., Van Brocklyn, J. R., Hobson, J. P., Movafagh, S., Zukowska-Grojec, Z., Milstien, S., and Spiegel, S. (1999) *J. Biol. Chem.* **274,** 35343–35350
12. Kovala, A. T., Harvey, K. A., McGlynn, P., Boguslawski, G., Garcia, J. G., and English, D. (2000) *FASEB J.* **14,** 2486–2494
13. Panetti, T. S., Nowlen, J., and Mosher, D. F. (2000) *Arterioscler. Thromb. Vasc. Biol.* **20,** 1013–1019
14. Matsuda, M., Tanaka, S., Nagata, S., Kojima, A., Kurata, T., and Shibuya, M. (1992) *Mol. Cell. Biol.* **12,** 3482–3489
15. Kiyokawa, E., Mochizuki, N., Kurata, T., and Matsuda, M. (1997) *Crit. Rev. Oncog.* **8,** 329–342
16. Klemke, R. L., Leng, J., Molander, R., Brooks, P. C., Vuori, K., and Cheresh, D. A. (1998) *J. Cell Biol.* **140,** 961–972
17. Cheresh, D. A., Leng, J., and Klemke, R. L. (1999) *J. Cell Biol.* **146,** 1107–1116
18. Kiyokawa, E., Hashimoto, Y., Kobayashi, S., Sugimura, H., Kurata, T., and Matsuda, M. (1998) *Genes Dev.* **12,** 3331–3336
19. Nishihara, H., Kobayashi, S., Hashimoto, Y., Ohba, F., Mochizuki, N., Kurata, T., Nagashima, K., and Matsuda, M. (1999) *Biochim. Biophys. Acta* **1452,** 179–187
20. Wu, Y. C., and Horvitz, H. R. (1998) *Nature* **392,** 501–504
21. Reddien, P. W., and Horvitz, H. R. (2000) *Nat. Cell Biol.* **2,** 131–136
22. Erickson, M. R., Galletta, B. J., and Abmayr, S. M. (1997) *J. Cell Biol.* **138,** 589–603
23. Stoletov, K. V., Ratcliffe, K. E., Spring, S. C., and Terman, B. I. (2001) *J. Biol. Chem.* **276,** 22748–22755
24. Hashimoto, Y., Katayama, H., Kiyokawa, E., Ota, S., Kurata, T., Gotoh, N., Otsuka, N., Shibata, M., and Matsuda, M. (1998) *J. Biol. Chem.* **273,** 17186–17191
25. Ribon, V., and Saltiel, A. R. (1996) *J. Biol. Chem.* **271,** 7375–7380
26. Rani, C. S., Wang, F., Fuior, E., Berger, A., Wu, J., Sturgill, T. W., Beitner-Johnson, D., LeRoith, D., Varticovski, L., and Spiegel, S. (1997) *J. Biol. Chem.* **272,** 10777–10783
27. Beitner-Johnson, D., and LeRoith, D. (1995) *J. Biol. Chem.* **270,** 5187–5190
28. Blakesley, V. A., Beitner-Johnson, D., Van Brocklyn, J. R., Rani, S., Shen-Orr, Z., Stannard, B. S., Spiegel, S., and LeRoith, D. (1997) *J. Biol. Chem.* **272,** 16211–16215
29. Waltenberger, J., Claesson-Welsh, L., Siegbahn, A., Shibuya, M., and Heldin, C. H. (1994) *J. Biol. Chem.* **269,** 26988–26995
30. Shibuya, M. (2001) *Cell Struct. Funct.* **26,** 25–35
31. He, H., Venema, V. J., Gu, X., Venema, R. C., Marrero, M. B., and Caldwell, R. B. (1999) *J. Biol. Chem.* **274,** 25130–25135
32. Takahashi, T., Yamaguchi, S., Chida, K., and Shibuya, M. (2001) *EMBO J.* **20,** 2768–2778
33. Dayanir, V., Meyer, R. D., Lashkari, K., and Rahimi, N. (2001) *J. Biol. Chem.* **276,** 17686–17692
34. Ito, N., Wernstedt, C., Engstrom, U., and Claesson-Welsh, L. (1998) *J. Biol. Chem.* **273,** 23410–23418
35. Levitzki, A., and Gazit, A. (1995) *Science* **267,** 1782–1788
36. Kovalenko, M., Gazit, A., Bohmer, A., Rorsman, C., Ronnstrand, L., Heldin, C. H., Waltenberger, J., Bohmer, F. D., and Levitzki, A. (1994) *Cancer Res.* **54,** 6106–6114
37. Strawn, L. M., McMahon, G., App, H., Schreck, R., Kuchler, W. R., Longhi, M. P., Hui, T. H., Tang, C., Levitzki, A., Gazit, A., Chen, I., Keri, G., Orfi, L., Risau, W., Flamme, I., Ullrich, A., Hirth, K. P., and Shawver, L. K. (1996) *Cancer Res.* **56,** 3540–3545
38. Sun, L., Tran, N., Tang, F., App, H., Hirth, P., McMahon, G., and Tang, C. (1998) *J. Med. Chem.* **41,** 2588–2603
39. Hennequin, L. F., Thomas, A. P., Johnstone, C., Stokes, E. S., Plè, P. A, Lohmann, J. J., Ogilvie, D. J., Dukes, M., Wedge, S. R., Curwen, J. O., Kendrew, J., and Lambert-van der Brempt, C. (1999) *J. Med. Chem.* **42,** 5369–5389
40. Hanke, J. H., Gardner, J. P., Dow, R. L., Changelian, P. S., Brissette, W. H., Weringer, E. J., Pollok, B. A., and Connelly, P. A. (1996) *J. Biol. Chem.* **271,** 695–701
41. Niwa, H., Yamamura, K., and Miyazaki, J. (1991) *Gene (Amst.)* **108,** 193–199
42. Ichiba, T., Hashimoto, Y., Nakaya, M., Kuraishi, Y., Tanaka, S., Kurata, T., Mochizuki, N., and Matsuda, M. (1999) *J. Biol. Chem.* **274,** 14376–14381
43. Kurokawa, K., Mochizuki, N., Ohba, Y., Mizuno, H., Miyawaki, A., and Matsuda, M. (2001) *J. Biol. Chem.* **276,** 31305–31310
44. Nishida, M., Maruyama, Y., Tanaka, R., Kontani, K., Nagao, T., and Kurose, H. (2000) *Nature* **408,** 492–495
45. Takayama, Y., Tanaka, S., Nagai, K., and Okada, M. (1999) *J. Biol. Chem.* **274,** 2291–2297
46. Ohba, Y., Ikuta, K., Ogura, A., Matsuda, J., Mochizuki, N., Nagashima, K., Kurokawa, K., Mayer, B. J., Maki, K., Miyazaki, J., and Matsuda, M. (2001) *EMBO J.* **20,** 3333–3341
47. Koch, W. J., Hawes, B. E., Inglese, J., Luttrell, L. M., and Lefkowitz, R. J. (1994) *J. Biol. Chem.* **269,** 6193–6197
48. Luttrell, L. M., Della Rocca, G. J., van Biesen, T., Luttrell, D. K., and Lefkowitz, R. J. (1997) *J. Biol. Chem.* **272,** 4637–4644
49. Daub, H., Wallasch, C., Lankenau, A., Herrlich, A., and Ullrich, A. (1997) *EMBO J.* **16,** 7032–7044
50. Ichiba, T., Kuraishi, Y., Sakai, O., Nagata, S., Groffen, J., Kurata, T., Hattori, S., and Matsuda, M. (1997) *J. Biol. Chem.* **272,** 22215–22220
51. Yancopoulos, G. D., Davis, S., Gale, N. W., Rudge, J. S., Wiegand, S. J., and Holash, J. (2000) *Nature* **407,** 242–248
52. Lee, M. J., Thangada, S., Claffey, K. P., Ancellin, N., Liu, C. H., Kluk, M., Volpi, M., Sha'afi, R. I., and Hla, T. (1999) *Cell* **99,** 301–312
53. Paik, J. H., Chae, S., Lee, M. J., Thangada, S., and Hla, T. (2001) *J. Biol. Chem.* **276,** 11830–11837
54. Windh, R. T., Lee, M. J., Hla, T., An, S., Barr, A. J., and Manning, D. R. (1999) *J. Biol. Chem.* **274,** 27351–27358
55. Prenzel, N., Zwick, E., Daub, H., Leserer, M., Abraham, R., Wallasch, C., and Ullrich, A. (1999) *Nature* **402,** 884–888
56. Daub, H., Weiss, F. U., Wallasch, C., and Ullrich, A. (1996) *Nature* **379,** 557–560
57. Heeneman, S., Haendeler, J., Saito, Y., Ishida, M., and Berk, B. C. (2000) *J. Biol. Chem.* **275,** 15926–15932
58. Oak, J. N., Lavine, N., and Van Tol, H. H. (2001) *Mol. Pharmacol.* **60,** 92–103
59. Eguchi, S., Dempsey, P. J., Frank, G. D., Motley, E. D., and Inagami, T. (2001) *J. Biol. Chem.* **276,** 7957–7962
60. Gille, H., Kowalski, J., Li, B., LeCouter, J., Moffat, B., Zioncheck, T. F., Pelletier, N., and Ferrara, N. (2001) *J. Biol. Chem.* **276,** 3222–3230

Carcinogenesis vol.23 no.4 pp.839–845, 2002

Deoxycholic acid causes DNA damage in colonic cells with subsequent induction of caspases, *COX-2* promoter activity and the transcription factors NF-kB and AP-1

B.Glinghammar, H.Inoue[1] and J.J.Rafter[2]

Department of Medical Nutrition, Karolinska Institutet, Novum, S-141 86 Huddinge, Sweden and [1]Department of Pharmacology, National Cardiovascular Center Research Institute, Osaka, Japan

[2]To whom correspondence should be addressed
Email: joseph.rafter@mednut.ki.se

Evidence is accumulating that bile acids induce apoptosis in colonic cells. Therefore, it becomes important to study the underlying molecular mechanisms and the role of this phenomenon in tumor promotion. Minutes after exposure of HCT 116 and HT-29 cells to deoxycholate (DCA), DNA damage, measured using the COMET assay, was evident. Caspase-3 was rapidly activated in HCT 116 cells exposed to DCA, whereas in HT-29 cells, caspase-3 activation was delayed. Using transient transfections with reporter constructs, we showed that the transcription factors activator protein-1 (AP-1) and NF-kB were increased in HCT 116 cells, in a dose-dependent fashion, by DCA *COX-2* promoter activity was also induced by DCA and using mutant *COX-2* promoter plasmids, we showed that the ability of DCA to induce promoter activity was partly dependent upon a functional NF-kB and C/EBP site, and completely dependent on a functional c-AMP response element site. DNA damage thus appears to be the initiating event in DCA-induced apoptosis. In conclusion, the bile acid, DCA, has a major impact on apoptotic mechanisms in colonic cells and this may be contributing to its effect as a tumor promoter.

Introduction

In colorectal cancer, genetic (1) and environmental factors contribute to the malignant transformation of colorectal epithelial cells. Epidemiological data implicate diet as a major environmental factor in colorectal carcinogenesis (2). A high fat consumption, seen in western societies, is associated with an increase in risk for colon cancer, as observed in many studies (3). One mechanism underlying this connection has been postulated to be increased levels of bile acids in the colon (4). Unconjugated deoxycholic acid (DCA) and chenodeoxycholic acid (CDCA) have been shown to be tumor promoters in animals (5,6) and higher levels of these bile acids have been reported in patients with adenomatous polyps and colon cancer (7,8). Earlier studies measured bile acids in total feces and attempted to correlate the levels to risk for colon cancer. However, more recently there has been a shift in focus towards the role of the aqueous phase of human feces (fecal water) in studies examining the mechanisms underlying the dietary etiology of colon cancer. The motivation for this is that components of this fecal fraction are more likely to be able to exert untoward effects on the cells of the colonic epithelium than components bound to food residues and the bacterial mass. The mechanism by which bile acids exert their tumor-promoting effect is poorly understood, although in recent years, many of the biological effects of bile acids at the molecular level are being clarified. Bile acids have, for example, been shown to activate protein kinase C (PKC) signaling pathways (9) involved in regulating cell proliferation, apoptosis and differentiation (10). DCA also induces *COX-2* promoter activity, which leads to the formation of the cyclooxygenase (COX)-2 enzyme and consequent increases in prostaglandin production (11). In animal studies, blocking COX-2 chemically or by mutation causes a marked decrease in colon cancer development (12,13). COX-2 is therefore a potential target for therapeutics.

In this paper, we have further investigated some DCA effects upon cultured colonic cells and studied some of the mechanisms underlying the stress response it induces in the cell. This was done by studying the effect of DCA upon transcription factors, such as activator protein-1 (AP-1) and NF-kB and the inducible gene, *COX-2*. We demonstrate that DCA induces apoptosis in colonic cells, and that caspase-3 activation differs markedly between different colonic cells. This process can be inhibited by blocking p38 or by binding up calcium in the cell. Protecting the DNA with spermine also reduces the activation of caspase-3, induced by DCA. Cells exposed to DCA show severely damaged DNA. The DNA damage precedes the apoptosis in time and may be the reason why the cell enters apoptosis (14).

Abbreviations: APC, adenomatous polyposis coli; AP-1, activator protein-1; CRE, c-AMP response element; COX, cyclooxygenase; DCA, deoxycholic acid; DMEM, Dulbecco's modified Eagle's medium; FBS, fetal bovine serum; PARP, poly-ADP-ribose polymerase; PKC, protein kinase C; TRE, TPA response element.

Material and methods

Chemicals

All chemicals were purchased from Calbiochem (Darmstadt, Germany) unless otherwise specified. DCA was prepared as stock solutions (0.1 mol/l) in water. SB 203580, BAPTA, PD98059, bisindolylmalemide, GO 6976, curcumin and apigenin were dissolved in dimethylsulfoxide. Spermine was dissolved in water.

Cells and culture

HT-29 and HCT 116 cell lines were purchased from ATCC (Rockville, MD) and used between passages 3 and 25 for all experiments. The HT-29 cell line is derived from a moderately well differentiated grade II human adenocarcinoma and is epithelial like. It harbors a mutated *APC* and expresses a truncated APC protein (15). HCT 116 cells are epithelial like and derived from a human carcinoma and harbor a normal *APC* gene (16). Both cells were maintained in Dulbecco's modified Eagle's medium (DMEM) with 10% fetal bovine serum (FBS), 2 mmol/l L-glutamine, 100 U/ml penicillin and 100 µg/ml streptomycin, in a humidified atmosphere of 95% air, 5% CO_2 at 37°C. They were subcultivated every week and given fresh medium every other day. To obtain quiescent cells for the procedures outlined below, cultures were serum starved [0% FBS, 0.2% lacto albumin hydrolysate (LAH)] for 24 h.

Assay for DNA damage

COMET assay

The method was basically that of Klaude *et al.* (17) with minor modifications. Clear microscope slides (Mentzel super frost, Kebo, Sweden) were pre-treated with 40 µl of 0.3% low melting point (LMP) agarose (type VII, Sigma, St Louis, MO) and allowed to air-dry. The cells were incubated with the test substance for 15 min at 37°C in a 5% CO_2 atmosphere. Ten microliters of

cell suspension ($0.5–1\times10^6$ cells/ml) was mixed with 150 µl of LMP agarose (0.75% in PBS kept at 37°C). A Flexi-Strip spatula was used to distribute the mixture on the pre-coated slides, which were thereafter left to set on an ice tray. After solidification, the slides were treated as follows. Lysis was performed in darkness for 1 h with an ice-cold freshly prepared solution containing 2 M NaCl, 25 mM EDTA, 20 mM Tris and 0.5% Triton X-100 pH 10. The slides were then placed in an electrophoresis buffer (0.3 M NaOH and 1 mM EDTA) in darkness at room temperature for 45 min. Electrophoresis was performed at room temperature, in darkness, in a Bio-Rad (Munich, Germany) subcell GT unit containing the same buffer, for 30 min at 20 V (0.67 V/cm). After electrophoresis, the slides were neutralized in 0.4 M Tris pH 7.4, air-dried, fixed in methanol and stored in a dry and dust free box until analysis. The DNA was stained with ethidium bromide (10 µg/ml in TAE) for 5 min followed by destaining for 5 min in TAE. The comets were examined in a fluorescence microscope (Olympus BH2 with a 20× apochromatic oil immersion objective), using the program Comet Assay II (Perceptive Instruments, Liverpool, UK). Images of 50 randomly selected cells were analyzed from each sample and tail moment was determined as described previously (18). Cell viability was assessed before and after the incubation by trypan blue exclusion.

Damage against DNA in vitro

c-DNA from a PCR reaction was incubated (37°C, 30 min) with PBS only or with DCA at increasing concentrations. The products were loaded onto an agarose gel stained with ethidium bromide (10 µg/ml in TAE) and subjected to electrophoresis for 1 h. The fluorescence from the bands was quantified in an imager (FUJI LAS 1000, Fuji, Stockholm, Sweden).

Caspase-3 assay

HCT 116 and HT-29 cells were grown to near confluence in 10 cm Petri dishes. Cells were washed with PBS and trypsinized. The pellet was resuspended in DMEM medium (0.1% FBS) and DCA at different concentrations was added and incubated for indicated time periods. After incubation, cells were centrifuged and the pellet was lyzed in a cell lysis buffer (10 mM Tris–HCl, 10 mM $NaH_2PO_4/NaHPO_4$ pH 7.5, 130 mM NaCl, 1% Triton X-100, 10mM $NaPP_i$). Protein concentration of the cell extract after centrifugation was measured with the Bradford method at 595 nm.

A 20 µl cell extract from each treatment was added to new tubes containing 250 µl HEPES buffer (40 mM HEPES pH 7.5, 20% glycerol, 4mM DTT) and 2.5 µl fluorogenic marker, DEVD-AMC [*N*-acetyl-Asp-Glu-Val-Asp-AMC (7-amino-4-methylcoumarin), Pharmingen, San Diego, CA]. After incubation for 1 h at 37°C, the mixture was excited at 380 nm in a spectrofluorometer and emission was detected at 400 nm.

Western blotting

HCT 116 and HT-29 cells were treated with DCA for indicated time periods. To study if poly-ADP-ribose polymerase (PARP) had been cleaved in the cells after DCA exposure, 20 µg whole cell extracts were subjected to SDS–polyacrylamide gel electrophoresis, which was performed under reducing conditions on 8% polyacrylamide as described by Laemmli (19). The resolved proteins were transferred to a nitrocellulose sheet as detailed by Towbin *et al.* (20) and subjected to Ponceaus staining. The nitrocellulose membrane was then incubated with mouse monoclonal antibodies against PARP (Pharmingen, San Diego, CA). The blots were probed with the corresponding secondary antibodies to IgG (Dakopatts, Stockholm, Sweden, 1:3000 dilution) conjugated to horseradish peroxidase. The ECL western blot detection system (Amersham, Buckinghamshire, UK) was used according to the manufacturer's instructions. The resulting bands were confirmed by comparing the size of the protein in the cell extract with known molecular markers (Bio-Rad Laboratories, Munchen, Germany).

Plasmid preparation

The *COX-2* promoter constructs (−1432/+59, −327/+59, −220/+59, −52/+59, CRM, KBM, ILM) were a kind gift from Drs Inoue and Tanabe (National Cardiovascular Center Research Institute, Osaka, Japan) (21,22). The reporter plasmids [TRE (TPA response element)$_3$tkLuc and (NF-kB)$_3$tkLuc were a gift from Dr Sam Okret (Karolinska Institute, Sweden) (23). The plasmid DNA was purified from bacteria cultures as described previously (24).

Transfection and luciferase assay

HCT 116 cells were grown to 50% confluence in a 75 cm^2 culture dish. The medium was removed and the cells were washed with PBS. OPTIMEM (Life Technologies, Gibco, Scotland, UK), 2 µg/ml plasmid DNA and 10 µg/ml Lipofectin reagent (Life Technologies) were added to the culture dish. After 6 h of transfection, the transfection mixture was removed and the cells were washed with PBS and trypsinized. Full growth medium (DMEM 10%) was then added to the cells to inhibit the trypsin, and the cells were pelleted by centrifugation at 2000 r.p.m. Cells (30×10^3) were seeded out in a 24 well plate, and DMEM 10% was added to each well and incubated overnight. The cells were then starved in DMEM (0.2% LAH) for 24 h, before being incubated with DCA for an additional 15 h. The medium was removed and the cells were washed with PBS. Lysis buffer (100 µl, 25 mmol/l trisphosphate pH 7.8, 15% glycerol, 2% CHAPS, 1% lecithin, 1% bovine serum albumin, 0.1% EGTA pH 8.0, 8 mmol/l $MgCl_2$, 1 mmol/l dithiothreitol and 0.4 mmol/l phenylmethylsulfonyl fluoride) was added to each well and the cells lysed during 30 min. A total of 50 µl of the cell lysates was transferred to a non-transparent 96 well plate and lucifierin mix (100 µl) (GenGlow, Bioorbit, Turku, Finland) was added per well. Assay for luciferase activity was performed in the automatic luminometer Lucy 1 (Anthos Labtec Instruments, Salzburg, Austria) according to the manufacturer's instructions. Luciferase activity was expressed per microgram of protein in the cell lysate. The luciferase activity of the untreated control cells in each experiment was set to 100% and the resulting activities for the test agents were calculated in relation (percent) to the control cells.

Cytotoxicity assay

Cell proliferation/toxicity using the HT-29 and HCT 116 cells was measured using the Celltiter 96 proliferation kit (Promega, Madison,WI) as described previously (24).

TUNEL assay

Apoptosis was evaluated using the TUNEL [Tdt (terminal deoxynucleotidyl transferase)-mediated dUTP-x (x = biotin, fluorescein) nick end labeling] assay (Böerhinger-Manheim, Indianapolis, IN) and flow cytometry analysis. Apoptotic DNA cleavage may yield single-stranded as well as double-stranded DNA breaks (nicks). Both types of breaks can be detected by labeling the 3′-OH termini with modified nucleotides (for example, fluorescein-dUTP) in an enzymatic reaction. Thus, 0.5×10^6 freshly harvested cells (attached + floating) were washed with PBS and fixed in 2% formaldehyde in PBS (1 ml) for 15 min at room temperature. Cells were washed with PBS and incubated with 0.1% saponine in balanced salt solution (4 ml) for 3 min. Subsequently, the cells were incubated with the TUNEL reaction mixture, 50 µl of enzyme solution (Tdt) and 450 µl of label solution (fluorescein d-UTP) for 1 h at 37°C in the dark in a humidified atmosphere. During this incubation period, Tdt catalyzes the addition of fluorescein-dUTP to free 3′-OH groups in single and double-stranded DNA. Omission of Tdt from the staining protocol constituted the negative control. After washing the cells with PBS, the label incorporated into the damaged sites of DNA was measured using a FACScan flow cytometer (Becton Dickinson, Mountain View, CA). For every experiment 10 000 cells were analyzed.

Statistics

In order to analyze changes in induction of *COX-2* promoter activity, AP-1- and NF-kB-dependent gene transcription, Student's *t*-test (two-tailed) was used. Pearson correlation was used to analyze correlations between variables. Descriptive and graphical methods were also used to characterize the data. All tests were performed with the software package STATISTICA 5.0 (Statsoft, Tulsa, OK) and the *P*-value is given for comparisons ($^*P < 0.05$, $^{**}P < 0.01$, $^{***}P < 0.001$).

Results

DCA induces DNA damage in intact cells but not on naked DNA

HCT 116 and HT-29 cells were exposed to DCA for 15 min at 37°C and analyzed for DNA damage using the single cell electrophoresis method. As seen in Figure 1A, DCA caused a significant increase in DNA strand breaks which were 3-fold higher ($P < 0.001$) than untreated cells for both HCT 116 and HT-29 cells. There was no difference in the DNA damage response between HT-29 and HCT 116 cells treated with DCA. In Figure 1B, DCA was incubated with naked DNA, for 30 min at 37°C, and the DNA products visualized on an agarose gel were quantified in an imager. DCA at 50–1000 µM did not have the capacity to break intact DNA *in vitro*.

Caspase-3 activation in HCT 116 and HT-29 cells after exposure to DCA

We and others, have shown previously that DCA induces apoptosis in cultured colonic cells (25,26). In order to further investigate how fast the apoptotic process is initiated we compared the activation of caspase-3 in two different cell lines, HCT 116 and HT-29. The cells were exposed to DCA

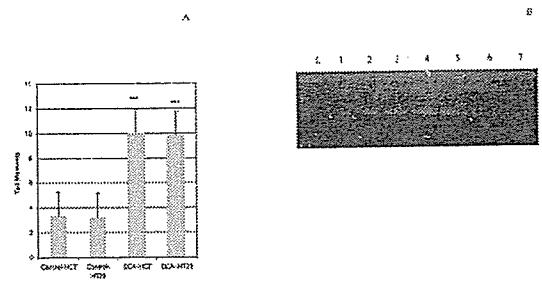

Fig. 1. (A) Measurement of DNA strand breaks in HCT 116 and HT-29 cells after exposure to DCA 500 μM (15 min). Bars represent mean tail moment ± SD (n = 50). (B) Intact DNA exposed to DCA (0–1000 μM) for 30 min at 37°C and visualized on an agarose gel. L, Ladder; lane 1, untreated DNA; lane 2, DCA 50 μM; lane 3, DCA 250 μM; lane 4, DCA 500 μM; lane 5, DCA 1000 μM; lane 6, positive control, 0.4% ammonium persulfate; lane 7, positive control, 0.8% ammonium persulfate.

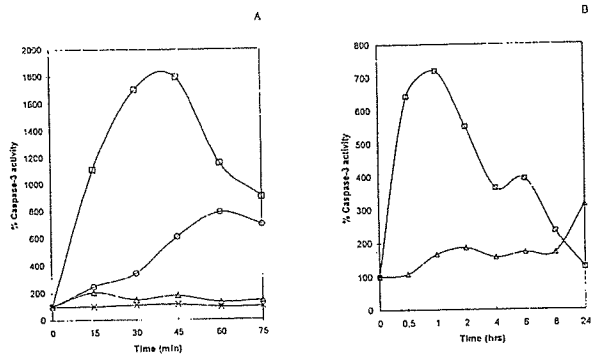

Fig. 2. (A) Dose-dependent effects of DCA on caspase-3 activity in HCT 116 and HT-29 cells after short-term treatment. HCT 116 cells: DCA 50 μM (triangle), DCA 250 μM (circle), DCA 500 μM (square); HT-29 cells: DCA 500 μM (cross). (B) Dose-dependent effects of DCA on caspase-3 activity in HCT 116 and HT-29 cells after long-term treatment. HCT 116: DCA 250 μM (squares). HT-29: DCA 250 μM (triangle).

at 50–500 μM from 0 to 75 min (Figure 2A). HCT 116 cells exposed to 50 μM DCA did not show any significant caspase-3 activity over the time period studied. DCA (250 μM) induced a dose-dependent activation of caspase-3 after 15 min, reaching a maximum after 60 min (800% above untreated cells). DCA (500 μM) induced a higher dose–response activation of caspase-3 and a maximum was reached after 45 min exposure (1800% above control). In HT-29 cells, no significant activation of caspase-3 was observed during this short-term exposure to DCA regardless of concentration used (50, 250 or 500 μM). In Figure 1A, only DCA 500 μM is plotted for the HT-29 cells. In Figure 2B, HCT 116 and HT-29 cells were treated with 250 μM DCA for 0.5, 1, 2, 4, 6, 8 and 24 h and activation of caspase-3 was studied. HCT 116 cells responded, as seen previously, with a rapid increase in caspase-3 activity, which reached a maximum after 60 min and then rapidly declined to basal levels after 24 h of treatment. In HT-29 cells, on the other hand, only a weak caspase-3 activity was observed after exposure to DCA for the earlier time points. However, after long-term exposure (24 h), the caspase-3 activity increased significantly (>300% above control, $P < 0.001$). The activation of caspase-3 by DCA in HT-29 cells was significantly delayed compared with HCT 116 cells, which may explain why HCT 116 cells are more sensitive to DCA than HT-29 cells [the numbers of surviving cells after 24 h exposure to

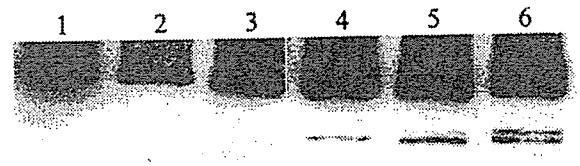

Fig. 3. Western blot, showing PARP protein (116 kDa) from cell extracts (HCT 116 cells) treated with DCA (250 μM) for 15–75 min. Lane 1, untreated 75 min; lane 2, 15 min treatment; lane 3, 30 min; lane 4, 45 min treatment; lane 5, 60 min treatment; lane 6, 75 min, treatment. The lower band appearing in lanes 4–6 represent cleaved PARP (85 kDa).

DCA (250 μM) are 48 ± 9 and 96 ± 15% for HCT 116 and HT-29, respectively, absorbance of untreated cells was set to 100%]. We also measured total cell death (cytotoxicity assay) in HT-29 cells exposed to DCA for 72 h and determined to what extent this was due to apoptosis (TUNEL assay). There was a linear correlation between total cell death and apoptosis (r = 0.96, $P < 0.001$) and the majority of the cell death was due to apoptosis (data not shown).

PARP cleavage in HCT 116 and HT-29 cells after DCA exposure

In order to study if protein substrates for caspase-3 in the cell are cleaved as rapidly as was observed in the *in vitro* system above, western blots on the same cell extracts (HCT 116, DCA 250 μM, 0–75 min) were performed and the membrane was probed with an antibody directed against the PARP protein. The result (Figure 3) shows PARP cleavage in the cell extracts (116 and 85 kDa) which correlates with cleavage of the fluorogenic marker, DEVD-AMC *in vitro* seen in Figure 2A. The protein fragment of PARP (85 kDa) was visible in cells which were treated with DCA (250 μM) for 45 min. In HT-29 cells, no cleavage of PARP was seen after these early time periods (0–75 min, data not shown). However, long-term exposure (up to 72 h) of HT-29 cells to DCA results in cleavage of PARP, which we have demonstrated previously (26).

Blocking of caspase-3 activation by inhibitors

Inhibitors were used in order to test if caspase-3 activity induced by DCA (500 μM) in HCT 116 cells could be prevented and to give some information about the signal transduction pathways involved. HCT 116 cells were used in these and subsequent experiments because of the larger and more rapid caspase response to DCA in these cells and the greater practical difficulties in transfecting the HT-29 cells. All inhibitors were pre-incubated for 15 min, before exposure to DCA. In Figure 4A, a dose-dependent inhibition of caspase-3 activity was observed when the cells had been pre-incubated with the antioxidant curcumin (10–50 μM). In a similar manner, the internal calcium chelator, BAPTA, was able to prevent caspase-3 from being activated. The PKC blocking agent (GO 6976, 50 nM) had no significant inhibitory effect on caspase-3 activity (Figure 4B). However, bisindolylmalemide (100 nM) had a partial blocking effect on caspase-3 activation by DCA. Interestingly, by blocking the stress-related map kinase, p38 (SB 203580, 30 μM), a complete suppression of caspase-3 activity was observed. Blocking MEK1/2 using PD98059 (10 μM) had, however, no effect on caspase-3 activation. The DNA protective amine, spermine (1 mM) could partially block induction of caspase-3 activation. Fifty percent of the actual apoptosis induced by DCA (500 μM) in HT-29 cells could be blocked by cell-permeable caspase-3 (Z-DEVD-FMK) and caspase 6 (Z-VEID-FMK) inhibitors at 100 μM

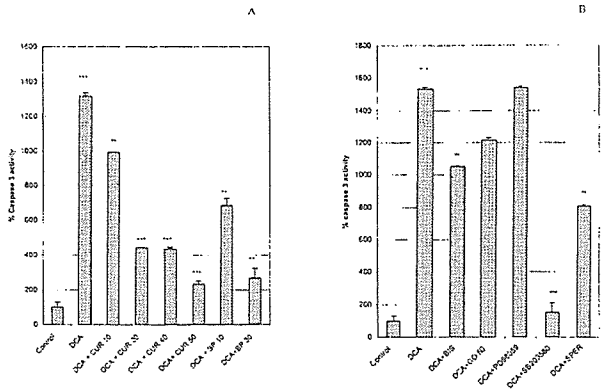

Fig. 4. (A) Caspase-3 activity in HCT 116 cells, treated with DCA (500 μM) for 30 min, with and without pre-treatment of inhibitors. CUR 10–CUR 50, curcumin 10–50 μM; BP 10–30, BAPTA 10–30 μM. (B) BIS, bisindolylmalemide 100 nM; GO, GO 6976 50 nM; PD, PD 98059 (10 μM); SB, SB 203580 (30 μM); SPER, spermine (1 mM). Bars represent mean ± SD (n = 2).

(A.Haza, Department of Medical Nutrition, Karolinska Institutet, personal communication).

Effects on NF-kB-dependent gene transcription by DCA

It has been reported previously that NF-kB is induced under cellular stress and NF-kB inhibitory effects on caspases have been described (27). It therefore became important to study if DCA induced NF-kB in HCT 116 cells.

HCT 116 cells were transiently transfected with a NF-kB-tk-luc plasmid and exposed to DCA at different concentrations for 15 h. Luciferase activity (Figure 5) was quantified and showed a dose-dependent increase in NF-kB-dependent gene transcription from 180% ($P < 0.05$) at DCA (100 μM) up to 300% induction ($P < 0.05$) at DCA (300 μM). DCA concentrations <100 μM did not induce the NF-kB-dependent gene transcription. TNF-α (400 U) was used as a positive control for induction of NF-kB-dependent gene transcription (Figure 5).

Inhibition of AP-1-dependent gene transcription induced by DCA

HCT 116 cells were transfected with a TRE-plasmid and exposed to DCA (250 μM) with and without inhibitors. The AP-1-dependent gene transcription was increased in HCT 116 cells in a dose-dependent fashion by DCA (Figure 6). Pre-treatment with GO 6976 (50 nM) had no significant effect upon AP-1-dependent gene transcription induced by DCA (250 μM) and neither had the MEK1/2 inhibitor, PD98059 (10 μM) or apigenin (20 μM). However, blocking the stress-related map kinase, p38, using SB 203580 (30 μM) totally abolished the AP-1-dependent gene transcription induced by DCA. Binding up calcium in the cell, using BAPTA (30 μM), also prevented AP-1 induction. Blocking PKC with bisindolylmalemide (100 nM) could partly prevent induction of AP-1. Curcumin (40 μM) completely abolished AP-1 induction induced by DCA.

Response elements in COX-2 promoter involved in trans-activation by DCA

We have shown previously that DCA induces the *COX-2* promoter in HCT 116 cells (28). The purpose of the present experiment was to understand what response elements in the *COX-2* promoter are involved in DCA induced transactivation.

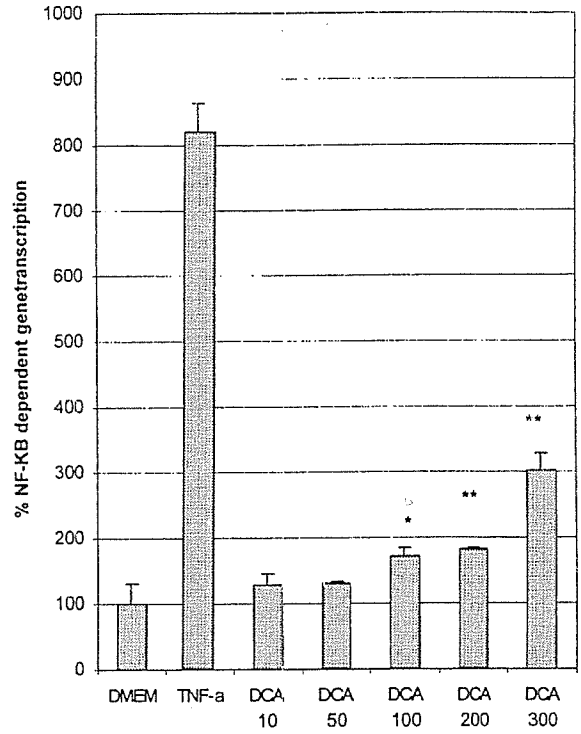

Fig. 5. Effects of DCA on NF-kB-dependent gene transcription in HCT 116 cells exposed to increasing concentrations of DCA for 15 h, before assay of luciferase activity. TNF-α, positive control. Bars represent mean ± SD (n = 4).

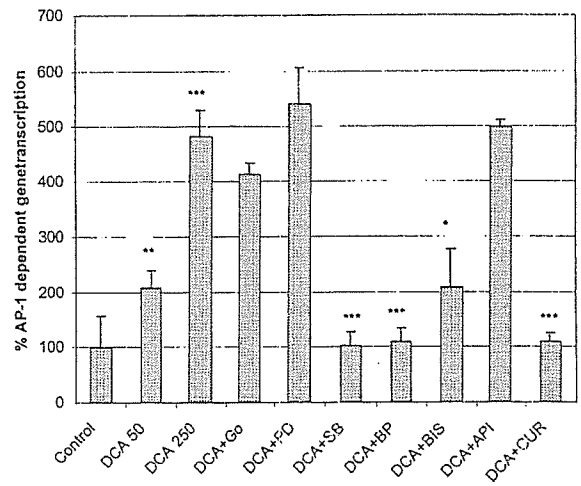

Fig. 6. Effects of DCA (250 μM) with and without inhibitors on AP-1-dependent gene transcription in HCT 116 cells. GO, GO 6976 50 nM; PD, PD 98059 10 μM; SB, SB 203580 30 μM; BP, BAPTA 30 μM; BIS, bisindolylmalemide 10 nM; API, apigenin 20 μM; CUR, curcumin 40 μM. Bars represent mean ± SD (n = 4).

Different lengths of the *COX-2* promoter plasmid were transiently transfected into HCT 116 cells and the cells were exposed to DCA 250 mM for 15 h. In Figure 7A, the full length *COX-2* promoter construct (–1432/+59), containing sites for SP1,

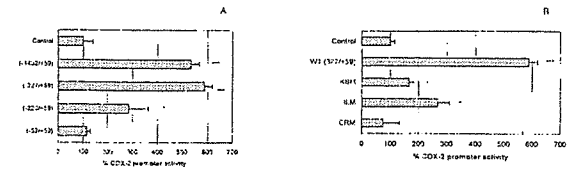

Fig. 7. (A) Deletion mutants of the *COX-2* promoter, transiently transfected into HCT 116 cells and exposed to DCA 250 μM for 15 h. –1432/+59 represents the *COX-2* plasmid, with 1432 bases upstream from the transcription start site of the *COX-2* promoter. (B) Mutants of the *COX-2* promoter plasmid, transiently transfected into HCT 116 cells and exposed to DCA 250 μM. KBM, represents the –327/+59 *COX-2* plasmid, with a mutation in the NF-kB site. ILM, represents the –327/+59 *COX-2* plasmid, with a mutation in the C/EBP site. CRM represents the –327/+59 *COX-2* plasmid, with a mutation in the CRE site. Bars represent mean ± SD (n = 8).

GRE, GATA, NF-kB, PEA3, SP1, NF-kB, AP-2, C/EBP and c-AMP response element (CRE) (29) induced a luciferase activity of 533 ± 33% above control (100%). The response of the deleted construct (–327/+59), containing sites for SP1, NF-kB, AP-2, C/EBP, CRE was of the same magnitude, 588 ± 32%. A clear reduction in response was observed with the (–220/+59) construct (AP-2, C/EBP, CRE), which gave an induction of 284 ± 80%. The shortest construct (–52/+59), lacking all response elements gave no induction compared with untreated cells (control).

In Figure 7B, the wild-type (–327/+59) plasmid, and mutated forms of the (–327/+59) plasmid were transfected into HCT 116 cells and exposed to DCA 250 μM. Using the KBM plasmid (–327/+59, NF-kB site mutated), resulted in a significant reduction in luciferase response compared with wild-type (–327/+59), 167 ± 17 and 588 ± 32%, respectively. Using the ILM plasmid (C/EBP mutation), a 50% reduction (269 ± 40%) was observed compared with the wild-type (–327/+59) construct. Comparing the CRM plasmid (CRE mutation) with the wild-type plasmid, a complete suppression of promoter activity was observed, 75 ± 58%.

Discussion

The precise mechanisms by which bile acids act as tumor promoters are not fully understood. Much work has focused upon the ability of bile acids to induce apoptosis in colonic cells, as a possible mechanism to explain its tumor-promoting effect in the colon (30). In this paper, we have studied the molecular effects resulting from exposure to DCA in the colonic cell lines HCT 116 and HT-29. The concentrations of DCA employed in the present study may seem to be high, but such concentrations have been reported to occur in the fecal water of risk groups for colon cancer (31,32). Shortly after exposure of these cells to DCA, when no cell death is evident, DNA damage can be detected. The mechanism behind damage of DNA after DCA exposure is not known. The fact that caspase-3 is rapidly induced in association with DNA damage and could be inhibited by DNA protective agents like spermine, supports the hypothesis that DNA damage may be inititating the apoptosis program. The antioxidant curcumin also reduced caspase-3 activity, which may indicate that DCA is provoking a free radical process in the cells that may lead to damage of the DNA. Stultz-Washo *et al.* (33) have shown that reactive nitrogen species are formed (peroxynitrite, coming from nitric oxide and superoxide) in HT-29 cells after DCA exposure (500 μM). The work by Craven *et al.* (34) has earlier shown that bile salt increases reactive oxygen production *in vivo*. Our observation that DCA did not have the capacity to induce damage to naked DNA *in vitro* also suggests that it is not DCA *per se* which is responsible for the damage, but rather a DCA-induced cellular process such as those mentioned above.

The activation of caspase-3 in HCT 116 and HT-29 cells differed markedly between the two cells after DCA exposure. There was a rapid and transient induction of caspase-3 activation upon DCA treatment (250 and 500 μM) in HCT 116 cells, and a delayed response (24 h) in HT-29 cells. This may be one explanation for our observation that HT-29 cells were more resistant than HCT 116 cells to cell death after 24 h exposure to DCA, despite equal damage to DNA induced by the bile acid. It is interesting to note that HCT 116 cells harbor normal *APC* and *p53* genes (15,35), both of which are mutated and non-functional in HT-29 cells (16,35). Both these genes are important for the initiation of the apoptosis program, and may contribute to explaining the difference observed between the two cell lines in the apoptosis response to DCA treatment (14,36).

DCA is inducing stress in the cells, and the stress-related map kinase, p38 is phosphorylated as shown previously (37). Interestingly, in our system blocking p38 could prevent caspase-3 activation induced by DCA. The activation of caspase-3 after DCA exposure seems to be calcium dependent, as the activation of caspase-3 could also be prevented by pre-incubation with BAPTA, an internal calcium chelator.

The results with the PKC inhibitors indicate that the induction of caspase-3 activity by bile acid is mediated, at least in part, by specific isoforms of PKC. Interestingly, blocking MEK1/2 had no effect on induction of caspase activity.

We measured the total cell death in HT-29 cells exposed to DCA at increasing concentrations, and in addition we quantified the number of apoptotic cells using the TUNEL staining. The result showed that there was a good correlation between the total cell death and apoptosis. At higher concentrations of DCA (>250 μM), the cell death was due to both necrosis and apoptosis; however, the majority of the cells were undergoing apoptosis. Evidence that DCA induces apoptosis *in vivo* under normal physiological conditions does exist. Perfusion studies in the rat colon have demonstrated that DCA has the capacity to induce the cell death referred to above (38).

Transfection of a NF-kB-tk-luc into HCT 116 cells and exposure (15 h) to increasing concentrations of DCA resulted in a dose-dependent increase of reporter gene activity, indicating that exposure to bile acid led to NF-kB activation. It is interesting, that the caspase-3 activity in the HCT 116 cells already after 15 h exposure to DCA had returned to basal levels. This becomes interesting, as it has been reported previously that NF-kB can inhibit caspase-3 activity via IAP activation (27). This may be interpreted as a survival mechanism, and is part of the cells response to the stress provoked by DCA. In transient transfection studies with a TRE-tk-luc plasmid in HCT 116 cells, DCA exposure resulted in a dose-dependent increase in AP-1-dependent gene transcription. This activation of AP-1 could be prevented by blocking p38, binding up calcium in the cells, as well as by the antioxidant curcumin. Blocking MEK1/2 had no effect, and results with PKC inhibitors indicated that the AP-1 activation

was mediated, at least in part, by specific PKC isoforms. There is a good correlation regarding the inhibitors that are needed to block activation of caspase-3- and AP-1-dependent gene transcription, which indicates that they are both part of the same stress response.

COX-2 is also involved in the stress response, and activity of COX-2 results in production of prostaglandins, which can make the cells more resistant to apoptosis (39). In order to elucidate the main transactivation domain in the *COX-2* promoter, we transfected the HCT 116 cells with different lengths of the *COX-2* promoter (luciferase reporter constructs) and exposed them to DCA. We observed that for the longer (–1432/+59) and the shorter (–327/+59) plasmid construct, there was no difference in reporter gene activity induced by DCA. However, between the (–327/+59) and (–220/+59) plasmid construct, there was a significant decrease in reporter gene activity. The difference between these two promoter constructs is that the (–220/+59) form lacks the NF-kB response element. Use of the shortest plasmid construct, (–52/+59), which only contains a TATA box, resulted in no induction by DCA compared with untreated cells. Using mutant (–327/+59) plasmids, we could demonstrate that a mutation in the NF-kB binding site significantly reduced the reporter gene activity compared with the response using wild-type (–327/+59). Mutation of the C/EBP binding site resulted in a 50% decrease in reporter gene activity. Finally, mutation of the CRE (c-AMP response element) totally abolished the reporter gene activity induced by DCA. In summary, the results indicate that DCA induction of the *COX-2* gene is complex, and involves multiple transcription factors binding to NF-kB, C/EBP and CRE elements. It is interesting to note that the CRE in the *COX-2* promoter is similar to a TRE element, and may bind AP-1 transcription factors as well as CREB factors/ATF (40). In addition, it has been demonstrated that C/EBP factors can also dimerize with AP-1 transcription factors (41). Our results are in agreement with those of Zhang *et al.* (11) who showed that DCA treatment of esophageal adenocarcinoma cells resulted in activation of the *COX-2* promoter. However, our results hopefully extend our understanding of bile acid induced signaling by mapping the response elements in the *COX-2* promoter that are required for full activation of gene transcription in colonic cells.

In conclusion, DCA induces apoptosis in HCT 116 and HT-29 cells, and cell death is delayed in HT-29 cells, which correlates with delayed activation of caspase-3. The activation of caspase-3 is dependent upon active p38 and normal calcium signaling. Cells undergoing DCA-induced apoptosis, but which are still viable have reduced caspase-3 levels and NF-kB and AP-1 are induced. In these cells, *COX-2* promoter activity is also induced, and mapping of the main transactivation domain, indicates that full activation of the promoter needs functional NF-kB, C/EBP and CRE elements located in the –327 bases up from start of transcription. Which transcription factors bind to these elements of the *COX-2* promoter when the cells are exposed to DCA is not fully elucidated and requires further investigation. Finally, the bile acid, DCA, has a major impact on the apoptotic machinery in colonic cells but the role of this effect in tumor promotion requires further work.

Acknowledgements

This work was supported by the Swedish Cancer Society. B.G. is grateful to Robert Lundbergs foundation for financial support.

References

1. Fearon.E.R. and Vogelstein.B. (1990) A genetic model for colorectal tumorigenesis. *Cell*, **61**, 759–767.
2. Sandler.R.S., Lyles.C.M., Peipins.L.A., McAuliffe.C.A., Woosley.J.T. and Kupper.L.L. (1993) Diet and risk of colorectal adenomas: macronutrients, cholesterol and fiber. *J. Natl Cancer Inst.*, **85**, 884–891.
3. Jenkins.D.J., Jenkins.A.L., Rao.A.V. and Thompson.L.U. (1986) Cancer risk: possible protective role of high carbohydrate high fiber diets. *Am. J. Gastroenterol.*, **81**, 931–935.
4. Weisburger.J.H., Reddy.B.S., Barnes.W.S. and Wynder.E.L. (1983) Bile acids, but not neutral sterols, are tumor promoters in the colon in man and in rodents. *Environ. Health Perspect.*, **50**, 101–107.
5. Reddy.B.S., Watanabe.K., Weisburger.J.H. and Wynder.E.L. (1977) Promoting effect of bile acids in colon carcinogenesis in germ-free and conventional F344 rats. *Cancer Res.*, **37**, 3238–3242.
6. Mahmoud.N.N., Dannenberg.A.J., Bilinski.R.T., Mestre.J.R., Chadburn.A., Churchill.M., Martucci.C. and Bertagnolli.M.M. (1999) Administration of an unconjugated bile acid increases duodenal tumors in a murine model of familial adenomatous polyposis. *Carcinogenesis*, **20**, 299–303.
7. Imray.C.H., Radley.S., Davis.A., Barker.G., Hendrickse.C.W., Donovan.I.A., Lawson.A.M., Baker.P.R. and Neoptolemos.J.P. (1992) Faecal unconjugated bile acids in patients with colorectal cancer or polyps. *Gut*, **33**, 1239–1245.
8. Reddy.B.S., Mastromarino.A., Gustafson.C., Lipkin.M. and Wynder.E.L. (1976) Fecal bile acids and neutral sterols in patients with familial polyposis. *Cancer*, **38**, 1694–1698.
9. Huang.X.P., Fan.X.T., Desjeux.J.F. and Castagna.M. (1992) Bile acids, non-phorbol-ester-type tumor promoters, stimulate the phosphorylation of protein kinase C substrates in human platelets and colon cell line HT29. *Int. J. Cancer.*, **52**, 444–450.
10. Clemens.M.J., Trayner.I. and Menaya.J. (1992) The role of protein kinase C isoenzymes in the regulation of cell proliferation and differentiation. *J. Cell Sci.*, **103**, 881–887.
11. Zhang.F., Subbaramaiah.K., Altorki.N. and Dannenberg.A.J. (1998) Dihydroxy bile acids activate the transcription of cyclooxygenase-2. *J. Biol. Chem.*, **273**, 2424–2428.
12. Oshima.M., Dinchuk.J.E., Kargman.S.L., Oshima.H., Hancock.B., Kwong.E., Trzaskos.J.M., Evans.J.F. and Taketo.M.M. (1996) Suppression of intestinal polyposis in Apc delta716 knockout mice by inhibition of cyclooxygenase 2 (COX-2). *Cell*, **87**, 803–809.
13. Jacoby.R.F., Seibert.K., Cole.C.E., Kelloff.G. and Lubet.R.A. (2000) The cyclooxygenase-2 inhibitor celecoxib is a potent preventive and therapeutic agent in the min mouse model of adenomatous polyposis. *Cancer Res.*, **60**, 5040–5044.
14. Rich.T., Allen.R.L. and Wyllie.A.H. (2000) Defying death after DNA damage. *Nature*, **407**, 777–783.
15. Hsi.L.C., Angerman-Stewart.J. and Eling.T.E. (1999) Introduction of full-length APC modulates cyclooxygenase-2 expression in HT-29 human colorectal carcinoma cells at the translational level. *Carcinogenesis*, **20**, 2045–2049.
16. Kutchera.W., Jones.D.A., Matsunami.N., Groden.J., McIntyre.T.M., Zimmerman.G.A., White.R.L. and Prescott.S.M. (1996) Prostaglandin H synthase 2 is expressed abnormally in human colon cancer: evidence for a transcriptional effect. *Proc. Natl Acad. Sci. USA*, **93**, 4816–4820.
17. Klaude.M., Eriksson.S., Nygren.J. and Ahnstrom.G. (1996) The comet assay: mechanisms and technical considerations. *Mutat. Res.*, **363**, 89–96.
18. Venturi.M., Hambly.R.J., Glinghammar.B., Rafter.J.J. and Rowland.I.R. (1997) Genotoxic activity in human faecal water and the role of bile acids: a study using the alkaline comet assay. *Carcinogenesis*, **18**, 2353–2359.
19. Laemmli.U.K. (1970) Cleavage of structural proteins during the assembly of the head of bacteriophage T4. *Nature*, **227**, 680–685.
20. Towbin.H., Staehelin.T. and Gordon.J. (1979) Electrophoretic transfer of proteins from polyacrylamide gels to nitrocellulose sheets: procedure and some applications. *Proc. Natl Acad. Sci. USA*, **76**, 4350–4354.
21. Inoue.H., Yokoyama.C., Hara.S., Tone.Y. and Tanabe.T. (1995) Transcriptional regulation of human prostaglandin-endoperoxide synthase-2 gene by lipopolysaccharide and phorbol ester in vascular endothelial cells. Involvement of both nuclear factor for interleukin-6 expression site and cAMP response element. *J. Biol. Chem.*, **270**, 24965–24871.
22. Inoue.H., Nanayama.T., Hara.S., Yokoyama.C. and Tanabe.T. (1994) The cyclic AMP response element plays an essential role in the expression of the human prostaglandin-endoperoxide synthase 2 gene in differentiated U937 monocytic cells. *FEBS Lett.*, **350**, 51–54.

23. Caldenhoven,E., Liden,J., Wissink,S., Van de Stolpe,A., Raaijmakers,J., Koenderman,L., Okret,S., Gustafsson,J.A. and Van der Saag,P.T. (1995) Negative cross-talk between RelA and the glucocorticoid receptor: a possible mechanism for the antiinflammatory action of glucocorticoids. *Mol. Endocrinol.*, **9**, 401–412.
24. Glinghammar,B., Holmberg,K. and Rafter,J. (1999) Effects of colonic lumenal components on AP-1-dependent gene transcription in cultured human colon carcinoma cells. *Carcinogenesis*, **20**, 969–976.
25. Hague,A., Elder,D.J., Hicks,D.J. and Paraskeva,C. (1995) Apoptosis in colorectal tumour cells: induction by the short chain fatty acids butyrate, propionate and acetate and by the bile salt deoxycholate. *Int. J. Cancer*, **60**, 400–406.
26. Haza,A.I., Glinghammar,B., Grandien,A. and Rafter,J. (2000) Effect of colonic luminal components on induction of apoptosis in human colonic cell lines. *Nutr. Cancer*, **36**, 79–89.
27. LaCasse,E.C., Baird,S., Korneluk,R.G. and MacKenzie,A.E. (1998) The inhibitors of apoptosis (IAPs) and their emerging role in cancer. *Oncogene*, **17**, 3247–3259.
28. Glinghammar,B. and Rafter,J. (2001) Colonic luminal contents induce cyclooxygenase 2 transcription in human colon carcinoma cells. *Gastroenterology*, **120**, 401–410.
29. Tazawa,R., Xu,X.M., Wu,K.K. and Wang,L.H. (1994) Characterization of the genomic structure, chromosomal location and promoter of human prostaglandin H synthase-2 gene. *Biochem. Biophys. Res. Commun.*, **203**, 190–199.
30. Payne,C.M., Bernstein,H., Bernstein,C. and Garewal,H. (1995) Role of apoptosis in biology and pathology: resistance to apoptosis in colon carcinogenesis. *Ultrastruct. Pathol.*, **19**, 221–248.
31. Ejderhamn,J., Rafter,J.J. and Strandvik,B. (1991) Faecal bile acid excretion in children with inflammatory bowel disease. *Gut*, **32**, 1346–1351.
32. de Kok,T.M., van Faassen,A., Glinghammar,B., Pachen,D.M., Eng,M., Rafter,J.J., Baeten,C.G., Engels,L.G. and Kleinjans,J.C. (1999) Bile acid concentrations, cytotoxicity and pH of fecal water from patients with colorectal adenomas. *Dig. Dis. Sci.*, **44**, 2218–2225.
33. Washo-Stultz,D., Hoglen,N., Bernstein,H., Bernstein,C. and Payne,C.M. (1999) Role of nitric oxide and peroxynitrite in bile salt-induced apoptosis: relevance to colon carcinogenesis. *Nutr. Cancer*, **35**, 180–188.
34. Craven,P.A., Pfanstiel,J. and DeRubertis,F.R. (1986) Role of reactive oxygen in bile salt stimulation of colonic epithelial proliferation. *J. Clin. Invest.*, **77**, 850–859.
35. Chendil,D., Oakes,R., Alcock,R.A., Patel,N., Mayhew,C., Mohiuddin,M., Gallicchio,V.S. and Ahmed,M.M. (2000) Low dose fractionated radiation enhances the radiosensitization effect of paclitaxel in colorectal tumor cells with mutant p53. *Cancer*, **89**, 1893–1900.
36. Browne,S.J., Williams,A.C., Hague,A., Butt,A.J. and Paraskeva,C. (1994) Loss of APC protein expressed by human colonic epithelial cells and the appearance of a specific low-molecular-weight form is associated with apoptosis *in vitro*. *Int. J. Cancer*, **59**, 56–64.
37. Qiao,D., Chen,W., Stratagoules,E.D. and Martinez,J.D. (2000) Bile acid-induced activation of activator protein-1 requires both extracellular signal-regulated kinase and protein kinase C signaling. *J. Biol. Chem.*, **275**, 15090–15098.
38. Rafter,J.J., Eng,W.W., Furrer,R., Medline,A. and Bruce,W.R. (1986) Effects of calcium and pH on the mucosal damage produced by deoxycholic acid in the rat colon. *Gut*, **27**, 1320–1329.
39. Tsujii,M. and DuBois,R.N. (1995) Alterations in cellular adhesion and apoptosis in epithelial cells overexpressing prostaglandin endoperoxide synthase 2. *Cell*, **83**, 493–501.
40. Nomura,N., Zu,Y.L., Maekawa,T., Tabata,S., Akiyama,T. and Ishii,S. (1993) Isolation and characterization of a novel member of the gene family encoding the cAMP response element-binding protein CRE-BP1. *J. Biol. Chem.*, **268**, 4259–4266.
41. Hsu,W., Kerppola,T.K., Chen,P.L., Curran,T. and Chen-Kiang,S. (1994) Fos and Jun repress transcription activation by NF-IL6 through association at the basic zipper region. *Mol. Cell. Biol.*, **14**, 268–276

Received June 22, 2001; and accepted January 14, 2002

Transcriptional and Posttranscriptional Regulation of Cyclooxygenase-2 Expression by Fluid Shear Stress in Vascular Endothelial Cells

Hiroyasu Inoue, Yoji Taba, Yoshikazu Miwa, Chiaki Yokota, Megumi Miyagi, Toshiyuki Sasaguri

Objective—Fluid shear stress induces cyclooxygenase (COX)-2 gene expression in vascular endothelial cells. We investigated the underlying mechanism of this induction.

Methods and Results—Exposure of human umbilical vein endothelial cells to laminar shear stress in the physiological range (1 to 30 dyne/cm^2) upregulated the expression of COX-2 but not COX-1, a constitutive isozyme of COX. The expression of COX-2 mRNA began to increase within 0.5 hour after the loading of shear stress and reached a maximal level at 4 hours. Roles of the promoter region and the 3′-untranslated region in the human COX-2 gene were evaluated by the transient transfection of luciferase reporter vectors into bovine arterial endothelial cells. Shear stress elevated luciferase activity via the region between −327 and 59 bp. Mutation analysis indicated that cAMP-responsive element (−59/−53 bp) was mainly involved in this response. On the other hand, shear stress selectively stabilized COX-2 mRNA. Moreover, shear stress elevated luciferase activity when a 3′-untranslated region of COX-2 gene containing 17 copies of the AUUUA mRNA instability motif was inserted into the vector.

Conclusions—Transcriptional activation and posttranscriptional mRNA stabilization contribute to the rapid and sustained expression of COX-2 in response to shear stress. (*Arterioscler Thromb Vasc Biol.* **2002;22:1415-1420.**)

Key Words: shear stress ■ vascular endothelial cells ■ cyclooxygenase-2 ■ posttranscriptional regulation

Vascular endothelial cells are always exposed to a wide variety of biochemical and biomechanical stimuli, including fluid shear stress caused by blood flow. Shear stress modulates several endothelial functions, such as control of vascular tone, maintenance of antithrombotic surfaces, regulation of inflammation, protection against oxidative stresses, and regulation of endothelial cell proliferation and apoptosis.[1]

Cyclooxygenase (COX), a rate-limiting enzyme for prostaglandin (PG) biosynthesis, comprises 2 isozymes, COX-1 and COX-2.[2,3] COX-1 is constitutively expressed in most cell species, whereas COX-2 is an inducible enzyme whose expression is regulated differently among cell types. Growing evidence indicates that COX-2 plays a key role in several biological processes, such as inflammation, tumorigenesis, development, and atherogenesis.[4–9] Laminar shear stress upregulates COX-2 gene expression.[10] COX-2 is involved in lipopolysaccharide-stimulated production of prostacyclin (PGI_2) in endothelial cells[11] and is also involved in PGI_2 biosynthesis in healthy humans.[12] Previously, we have reported that shear stress promotes the production of PGD_2 in endothelial cells by stimulating the expression of lipocalin-type PGD_2 synthase (L-PGDS), whereas PGI_2 synthase was constitutively expressed but did not respond to shear stress.[13] Therefore, the induction of COX-2 expression by shear stress may be involved in the production of PGI_2 and PGD_2 in endothelial cells.

Three *cis*-acting elements, namely, the nuclear factor (NF)-κB binding site, the NF–interleukin-6 (NF-IL6) binding site, and the cAMP-responsive element (CRE), reside in the region between base pairs −327 and +59 (−327/+59) in the human COX-2 gene promoter. Their involvement in COX-2 gene transcription varies among cell species.[14–24] Recently, the COX-2 gene has been reported to be posttranscriptionally regulated through its 3′-untranslated region (3′-UTR) containing 17 copies of the AUUUA motif, which is assumed to promote mRNA degradation.[25–30] However, the mechanism underlying shear stress–induced COX-2 gene expression remains to be elucidated, although it has been recently reported that shear stress stimulates the transcription of the COX-2 gene in murine osteoblastic MC3T3-E1 cells that produce PGE_2 but not PGI_2 or PGD_2.[24]

In the present study, we investigated the molecular mechanism for the shear stress–induced expression of COX-2 in vascular endothelial cells. The gene expression of COX-2 was more sensitive to shear strength than that of L-PGDS. We found that shear stress induces COX-2 expression not only at

Received March 4, 2002; revision accepted June 20, 2002.

From the Departments of Pharmacology (H.I.), Bioscience (Y.M.), and Etiology and Pathogenesis (C.Y.), National Cardiovascular Center Research Institute, Osaka, and the Department of Clinical Pharmacology (Y.T., M.M., T.S.), Graduate School of Medical Sciences, Kyushu University, Fukuoka, Japan.

Correspondence to Hiroyasu Inoue, PhD, Department of Pharmacology, National Cardiovascular Center Research Institute, 5-7-1 Fujishiro-dai, Suita, Osaka 565-8565, Japan. E-mail inoue@ri.ncvc.go.jp

Arterioscler Thromb Vasc Biol. is available at http://www.atvbaha.org

DOI: 10.1161/01.ATV.0000028816.13582.13

the transcriptional level but also at the posttranscriptional level through the 3′-UTR, which would make it possible to rapidly and persistently induce COX-2 expression in response to shear stress.

Methods

Cell Culture

Human umbilical vein endothelial cells (HUVECs) were isolated and cultured as described.[31] Bovine arterial endothelial cells (BAECs) were grown in DMEM supplemented with 10% FCS (Flow), 100 U/mL penicillin, and 100 μg/mL streptomycin.[16]

Shear Stress Apparatus

HUVECs and BAECs were plated on a gelatin-coated polyester sheet (Plastic Suppliers), and flow experiments were performed in a parallel-plate flow chamber as described.[32]

Western Blot Analysis and Electrophoretic Mobility Shift Assay

Western blot analysis and electrophoretic mobility assay were performed as described.[16,23]

RNA Analysis

Total RNA was isolated by using the acid guanidinium thiocyanate procedure. RNAs were then subjected to electrophoresis. The cDNA probes for COX-1, COX-2, and GAPDH have been described previously.[16] The levels of mRNA and 28S rRNA were calculated on the basis of hybridization signals and ethidium bromide–staining intensities as measured with the imaging analyzers Fujix BAS 2500 and FLA 2000, respectively (Fuji Photo Film Co).

Plasmid Construction

The following control vectors were used: for luciferase (Luc), pGV-C (Toyo); for β-galactosidase (β-gal), pCMV-βgal; and for green fluorescent protein (GFP), pEGFP-N1 (Clontech).[11] The human COX-2 genomic clone λhPESII95 was digested by *Eco*RI, and then these fragments were subcloned into pBluescript II SK(+). Digestion of the subclone 7k1-2 with *Mro*I and *Eco*RI yielded a fragment containing part of the coding region (57 bp) and the full-length 3′-UTR, which contains 17 copies of the ATTTA motif followed by 3 copies of the polyadenylation signal (AATAAA).[33] This fragment was blunted and ligated into the blunted–*Pfl*M I site of pGV-C, which is located downstream from the Luc coding region. In this clone, designated pG-3UCOX2, Luc mRNA is expressed under the control of the SV40 enhancer/promoter and the 3′-UTR of the human COX-2 gene. Construction of other COX-2 reporters has been described previously.[11,16]

Transcription Assays

Transfection of BAECs with plasmids has been described previously.[11] In this experiment, 200 μL DMEM containing 2 μg COX-2 Luc reporter vector, 0.2 μg pCMV-βgal, and 0.1 μg pEGFP-N1 was mixed with 200 μL DMEM containing 10 μL Trans IT-LT-1 (Pan Vera) and incubated at room temperature for 15 minutes. This DNA/reagent complex was added to semiconfluent BAECs growing in a 90-mm dish containing 8 mL complete growth medium that was changed 1 day before the transfection. After 5 hours of transfection, cells were incubated with new complete growth medium for 19 hours and placed in the flow shear stress chamber. After incubation in the chamber for 24 hours, cells were subjected to fluid shear stress for 5 or 17 hours by using the apparatus described above. The cells were lysed in Reporter lysis buffer (Promega) to release the Luc and β-gal for their activity assays. The numerical readings from the Luc assay were normalized to those of the β-gal assay.[16]

Statistical Analysis

Results are expressed as mean±SD. Statistical significance was assessed by the Student *t* test.

Results

Laminar Shear Stress Induces COX-2 Expression in HUVECs

To determine the effect of shear stress on the expression of COX genes, we performed Western and Northern blot analyses with the use of protein and RNA extracted from HUVECs. COX-2 protein was expressed after the loading of shear stress (15 dyne/cm^2) for 24 hours but not in cells cultured under static conditions (please see online Figure IA, available at http://atvb.ahajournals.org). As shown in Figure 1A, the expression levels of COX-2 mRNA were very low under static conditions. Exposure of the cells to shear stress (15 dyne/cm^2) for the periods indicated led to an increase in the amount of COX-2 mRNA. On the other hand, COX-1 mRNA was constitutively expressed independently of shear stress. Because the expression level of COX-2 mRNA reached an almost maximal value at 6 hours, we further examined the time course of COX-2 induction immediately after loading shear stress (Figure 1B and online Figure IB). The level of COX-2 mRNA began to increase within 0.5 hours and reached a plateau at 4 hours.

Figure 2 shows the dependence of the expression of COX-2 mRNA on the strength of shear stress. The expression of COX-2 mRNA was maximally upregulated even at 5 dyne/cm^2, which corresponds to the level of shear stress in veins. Therefore, we performed an additional experiment to determine whether shear stress <5 dyne/cm^2 is able to stimulate COX-2 expression. As shown in Figure 2A, shear stress as low as 1 dyne/cm^2 significantly upregulated the expression.

Laminar Shear Stress Activates COX-2 Promoter

To examine whether shear stress stimulates the human COX-2 promoter, we used phPES2 (−327/+59), a plasmid that expresses firefly Luc under the control of the human COX-2 gene promoter (−327/+59). Because DNA transfection efficiency was much higher in BAECs than in HUVECs, phPES2 (−327/+59) was transfected into BAECs. Online Figure IIA (available at http://atvb.ahajournals.org) demonstrates BAECs transfected with pEGFP-N1, a GFP expression plasmid. The transfection efficiency seemed to be sufficient, and shear stress induced cell elongation along with the flow direction, which indicated that shear stress was successfully loaded on the cells. Moreover, that bovine COX-2 mRNA expression is also inducible in response to shear stress was confirmed by Northern blotting, as shown in online Figure IIB. Bovine COX-2 mRNA was induced by shear stress after 5 and 17 hours in duplicate experiments with independent materials. However, bovine COX-1 mRNA was not induced, again similar to human COX-1. As shown in online Figure IIC, the promoter activity of phPES2 (−327/+59) was markedly elevated by shear stress loaded for 5 and 17 hours.

The human COX-2 promoter region (−327/+59) contains 3 *cis*-acting elements, namely, an NF-κB binding site, an NF-IL6 binding site, and a CRE, all of which have been

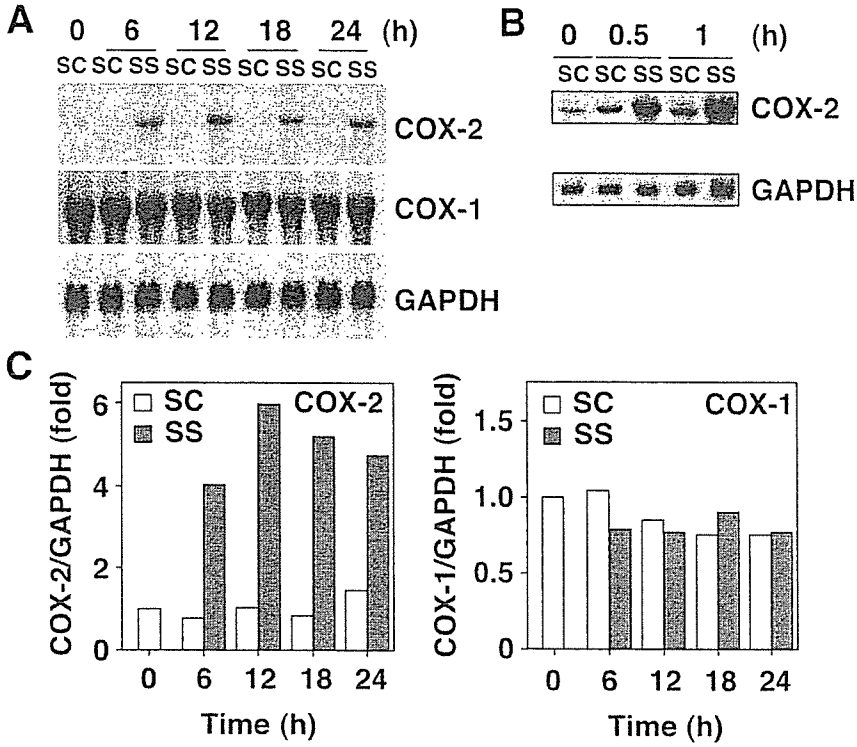

Figure 1. Shear stress (SS) induces the expression of COX-2 but not COX-1 in HUVECs. A, After exposing endothelial cells to SS (15 dyne/cm^2), total cellular RNAs were extracted at the time indicated. A and B, RNAs (10 μg per lane) were analyzed by RNA blot analysis for COX-2, COX-1 (panel A only), and GAPDH. SC indicates static control. Imaging-exposure times for panels A and B were 1 day and 5 days, respectively. C, Data obtained in panel A were quantified. Expression levels of COX-2 and COX-1 mRNAs normalized with those of GAPDH mRNA were standardized to the value obtained at 0 hour and are shown as fold increases. Similar results were obtained by 2 additional experiments.

shown to be involved in the regulation of COX-2 gene transcription. When we destroyed all of the 3 consensus sequences as shown in Figure 3A, the shear stress–induced elevation of the promoter activity completely disappeared, suggesting that the elements responsive to shear stress are in these 3 consensus sites. To identify the elements, we then destroyed each of the 3 motifs as shown in Figure 3B. A mutation in CRE (−59/−53) markedly reduced the basal and shear stress–induced promoter activities. Mutations at the NF-κB site (−223/−214) or NF-IL6 site (−132/−124) did not affect the response to shear stress compared with effects of the CRE, although the basal promoter activity was significantly reduced by the NF-IL6 mutation and tended to be reduced by the NF-κB mutation. Electrophoretic mobility shift assay showed that proteins specifically binding to the CRE (−59/−53) were enhanced by the shear stress (see online Figure III, available at http://atvb.ahajournals.org). These data suggest that the CRE (−59/−53) is mainly involved in the shear stress–increased COX-2 promoter activity.

Laminar Shear Stress Stabilizes COX-2 mRNA Through 3′-UTR

To examine whether posttranscriptional mechanisms are involved in shear stress–induced COX-2 expression, we chased the decay of COX-2 mRNA after the addition of actinomycin D, an inhibitor of transcription. As shown in Figure 4, COX-2 mRNA increased by shear stress loaded for 2 hours was almost completely degraded 2 hours after the addition of actinomycin D in the absence of stress. However, when shear stress was loaded simultaneously with actinomycin D, the decay of COX-2 mRNA was significantly delayed, and the enhanced expression was still retained at 4 hours after the addition of actinomycin D.

The entire 3′-UTR of the human COX-2 gene contains 17 copies of the ATTTA motif, which is found in many immediate-early genes and has been shown to promote mRNA degradation.[34,35] To determine whether the 3′-UTR of COX-2 mediates shear stress–induced mRNA stabilization, we examined the effect of the insertion of the COX-2 3′-UTR into the Luc expression vector. As shown in Figure 5, transfection of pG-3UCOX2 resulted in an ≈50% reduction in the promoter activity compared with that of pGV-C in cells cultured under static conditions, suggesting that the 3′-UTR of COX-2 destabilized the Luc mRNA. Shear stress did not influence the Luc activity in cells transfected with pGV-C, whereas it markedly elevated the activity by 2.8-fold in cells transfected with pG-3UCOX2. This suggested that exposure to laminar shear stress prevented Luc mRNA breakdown through the 3′-UTR of the COX-2 gene.

Discussion

The present study demonstrated for the first time that laminar shear stress within the physiological range induces COX-2 gene expression through transcriptional and posttranscriptional mechanisms in vascular endothelial cells. Shear stress as low as 1 dyne/cm^2 was able to induce COX-2 mRNA expression in HUVECs, as in murine osteoblastic MC3T3-E1 cells.[24] However, it was not able to stimulate COX-1 mRNA expression in either HUVECs or BAECs. A similar result, ie, that laminar shear stress induced COX-2 but not COX-1 expression, has been reported in a study using HUVECs,[10] although higher shear stress (24 dyne/cm^2) has been reported to induce COX-1 mRNA in HUVECs,[36] and mechanical cyclic strain also has been shown to induce COX-1 in human

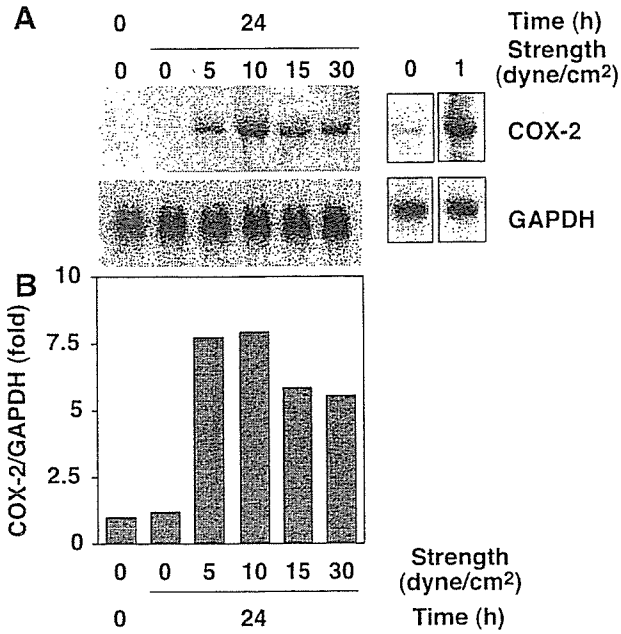

Figure 2. Effect of shear strength on induction of COX-2 mRNA expression in HUVECs. A, HUVECs were exposed to various levels of shear stress (0 to 30 dyne/cm^2) for 24 hours. Total cellular RNAs (10 μg per lane) were analyzed by RNA blot analysis for COX-2 and GAPDH. Imaging-exposure times for the left and right parts were 1 day and 5 days, respectively. B, Data obtained in panel A was quantified. Expression levels of COX-2 normalized to those of GAPDH mRNA are shown as the fold increase against the value obtained at time 0. Similar results were obtained by 2 additional experiments.

vascular smooth muscle cells.[37] COX-2 has been reported to have a higher affinity for arachidonate than COX-1,[38] and moreover, COX-2 preferentially cooperates more with PGI_2 synthase than with COX-1.[39] When these findings are taken together, COX-2 but not COX-1 appears to be mainly involved in PGI_2 formation in blood vessels loaded with laminar shear stress in the physiological range. This assumption is consistent with recent studies reporting that selective COX-2 inhibitors suppress the systemic biosynthesis of PGI_2 in healthy humans[12] and in patients with atherosclerosis.[40] There has been a report that glucocorticoids do not depress the excretion of urinary PGI_2 metabolite.[41] We found that COX-2 expression was not suppressed by dexamethasone, especially in vascular endothelial cells, because of the lower expression of the glucocorticoid receptor.[11] There are variable reports of COX-2 expression ex vivo in endothelial cells. It will be difficult to evaluate the precise expression levels of COX-2 ex vivo after postmortem examination because COX-2 mRNA and protein are very unstable.

We reported that laminar shear stress also induces the expression of L-PGDS.[13] However, the induction of gene expression by shear stress was more rapid and sensitive for COX-2 than for L-PGDS, whose mRNA expression increases depending on shear strength between 5 and 30 dyne/cm^2. PGI_2 synthase is constitutively expressed in endothelial cells, and its expression level is not influenced by shear stress.[13] Therefore, we hypothesize that there are 2 steps in COX-2–mediated arachidonate metabolism in endothelial cells. Step 1, which operates under low shear stress conditions, predominantly produces PGI_2, and step 2, which operates under high shear stress conditions, produces not only PGI_2 but also PGD_2. In this context, PGD_2 may also play a role in preventing the formation of atherosclerotic lesions by being converted to 15-deoxy-$\Delta^{12,14}$-PGJ_2, which has been reported to display several antiatherogenic effects on cultured vascular cells.[42]

In the mean time, macrophages were reported to express augmented levels of COX-2 in atherosclerotic lesions.[43,44] This abnormally elevated COX-2 expression in macrophages may be related to inflammation in the lesions. Because the PGs produced in macrophages are different from those produced in endothelial cells, the regulation of COX-2 and downstream enzymes should be very different between endothelial cells and macrophages. In this context, we have recently reported that COX-2 expression is negatively regulated by nuclear receptor peroxisome proliferator–activated receptor-γ and its ligand candidate 15-deoxy-$\Delta^{12,14}$-PGJ_2 in macrophages but not in endothelial cells.[23] Whether changes

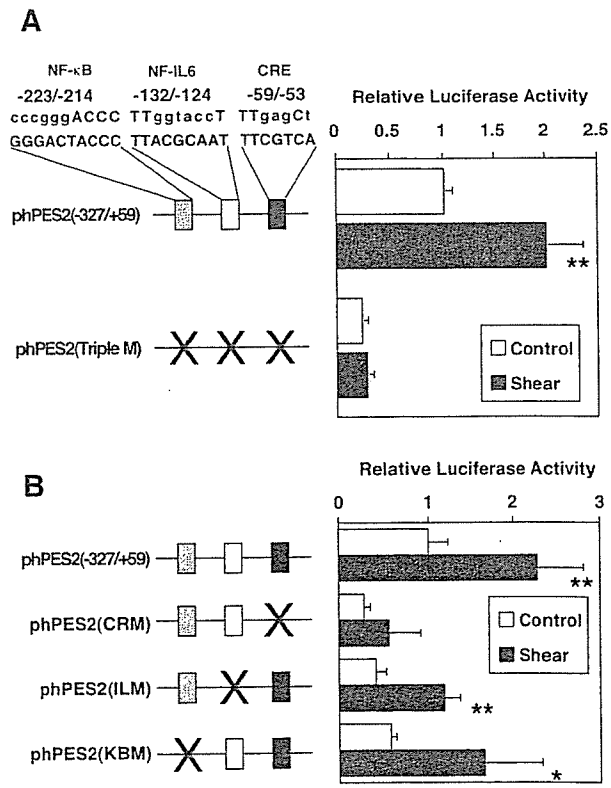

Figure 3. Site-specific mutation of the COX-2 promoter region in response to shear stress. The human COX-2 gene promoter (−327/+59) was mutated at each putative transcriptional regulatory element. Lowercase letters in the upper sequence of each promoter indicate mutated bases, and the lower sequence shows wild-type bases. BAECs were transiently transfected with the wild-type and mutated constructs along with pCMV-βgal and pEGFP-N1. The transfected cells were subjected or not to shear stress at 15 dynes/cm^2 for 17 hours and then assayed for Luc and β-gal activities. The Luc activity was normalized to the β-gal activity and presented as the fold increase against the value obtained without shear stress of phPES2 (−327/+59). Data are mean±SD of 3 or 4 experiments. *P<0.05 vs static control; **P<0.01 vs static control.